© 2015. Published by The Company of Biologists Ltd | Journal of Cell Science (2015) 128, 3068-3081 doi:10.1242/jcs.170092

RESEARCH ARTICLE

The late endocytic Rab39a GTPase regulates the interaction between multivesicular bodies and chlamydial inclusions

Julian Gambarte Tudela[1], Anahi Capmany[1], Maryse Romao[2], Cristian Quintero[1], Stephanie Miserey-Lenkei[3], Graca Raposo[2], Bruno Goud[3] and Maria Teresa Damiani[1,*]

ABSTRACT

Given their obligate intracellular lifestyle, *Chlamydia trachomatis* ensure that they have access to multiple host sources of essential lipids by interfering with vesicular transport. These bacteria hijack Rab6-, Rab11- and Rab14-controlled trafficking pathways to acquire sphingomyelin from the Golgi complex. Another important source of sphingolipids, phospholipids and cholesterol are multivesicular bodies (MVBs). Despite their participation in chlamydial inclusion development and bacterial replication, the molecular mechanisms mediating the interaction between MVBs and chlamydial inclusions remain unknown. In the present study, we demonstrate that Rab39a labels a subset of late endocytic vesicles – mainly MVBs – that move along microtubules. Moreover, Rab39a is actively recruited to chlamydial inclusions throughout the pathogen life cycle by a bacterial-driven process that depends on the Rab39a GTP- or GDP-binding state. Interestingly, Rab39a participates in the delivery of MVBs and host sphingolipids to maturing chlamydial inclusions, thereby promoting inclusion growth and bacterial development. Taken together, our findings indicate that Rab39a favours chlamydial replication and infectivity. This is the first report showing that a late endocytic Rab GTPase is involved in chlamydial infection development.

KEY WORDS: *Chlamydia trachomatis*, Rab, Rab39a, Multivesicular bodies, Pathogen–host-cell interaction, Lipid transport

INTRODUCTION

Infections caused by *Chlamydia trachomatis* have a substantial impact on public health. Recurring chlamydial infections can lead to permanent sequelae such as blinding trachoma and female infertility. This widely spread human pathogen is an obligate intracellular Gram-negative bacterium, which undergoes its entire life cycle inside a vacuole called an inclusion. The infectious cycle starts with the attachment of the elementary body – the infectious bacterial form – to the host epithelial cell. This is followed by the triggering of a signalling cascade that culminates with the internalization of the bacterium. Once inside the host cell, the elementary body rapidly differentiates into the metabolically active, but non-infectious, bacterial form known as the reticulate body. Inclusion growth and bacterial replication depends on the acquisition of nutrients and biosynthetic constituents from the host. Following multiple rounds of replication, reticulate bodies re-differentiate back into elementary bodies and leave infected cells by lysis or extrusion, after which bacteria disseminate and invade neighbouring cells (Bastidas et al., 2013; Damiani et al., 2014).

The success of this pathogen resides in the relationship with the infected cell. To date, the molecular players mediating this pathogen–host interaction remain largely unknown. It is thought that chlamydial effectors exposed at the inclusion membrane, named Inc proteins, participate in the interplay between the bacteria and the host cell (Betts et al., 2009; Dehoux et al., 2011; Valdivia, 2008). However, it is unclear how these bacterial molecules infringe on host cell functioning. Furthermore, very little is known about how *C. trachomatis* co-opts the host cell protein machinery to ensure its survival and replication.

C. trachomatis growth and replication rely heavily upon the acquisition of certain lipids, mainly sphingolipids and cholesterol, from eukaryotic host cells (Saka and Valdivia, 2010). Interestingly, *C. trachomatis* acquire lipids through non-vesicular and vesicular mechanisms: (1) by recruiting transporters and synthases from host cytosolic sphingolipid factories at the boundaries of inclusions (Derré et al., 2011; Elwell et al., 2011) and (2) from Golgi-derived exocytic vesicles and multivesicular bodies (MVBs) (Beatty, 2006; Cocchiaro et al., 2008; Hackstadt et al., 1996; Moore et al., 2008).

MVBs are organelles that are strategically located at the intersection of endocytic and exocytic pathways. In addition to their pivotal role in exogenous material sorting, MVBs are potential intermediates in the transport of Golgi-derived vesicles (Denzer et al., 2000; Huotari and Helenius, 2011; Piper and Katzmann, 2007; Stoorvogel et al., 2002; Woodman and Futter, 2008). Particularly abundant in sphingolipids, lysobisphosphatidic acid (LBPA) and cholesterol, MVBs are a main source of host lipids hijacked by bacteria (Beatty, 2006, 2008; Robertson et al., 2009). Despite the importance of these late endocytic organelles for chlamydial development, the host protein machinery exploited by these bacteria to promote MVB–inclusion interaction is currently unknown.

Rab proteins (hereafter referred to as 'Rabs') are the largest family in the Ras-like small GTPase super family and tightly control vesicular trafficking. There are more than 60 distinct Rabs in mammalian cells and each one regulates a particular transport event. Rabs regulate sorting and budding from donor compartments, vesicular movement on cytoskeleton trails, proper targeting of vesicles, and docking and fusion with acceptor partners. These GTPases act as molecular switches, cycling between an inactive GDP-bound state and an active GTP-bound form, that latter of which is engaged with its specific target membrane (Ali and Seabra, 2005; Stenmark, 2009; Zerial and McBride, 2001). A few reports have investigated the localization of Rabs on MVBs, primarily identifying Rab7 and Rab11 (Fukuda et al., 2008; Savina et al., 2005).

[1]Laboratory of Phagocytosis and Intracellular Transport, School of Medicine, University of Cuyo, IHEM-CONICET, Mendoza 5500, Argentina. [2]Structure and Membrane Compartments, Cell and Tissue Imaging Facility, CNRS UMR144, Curie Institute, Paris 75248, France. [3]Molecular Mechanisms of Intracellular Transport, CNRS UMR144, Curie Institute, Paris, France.

*Author for correspondence (meteresadamiani@gmail.com)

Received 11 February 2015; Accepted 6 July 2015

Journal of Cell Science (2015) 128, 3068-3081 doi:10.1242/jcs.170092

C. trachomatis interfere with the host Rab-dependent vesicular trafficking pathways in order to generate hospitable intracellular conditions for bacterial survival and multiplication (Rzomp et al., 2003). By avoiding the interaction with Rab5 and Rab7, *C. trachomatis* escape from degradation in the phagocytic pathway (Fields and Hackstadt, 2002). In contrast, recruitment of Rab6 (Rejman Lipinski et al., 2009), Rab11 (Leiva et al., 2013; Rejman Lipinski et al., 2009) and Rab14 (Capmany and Damiani, 2010; Capmany et al., 2011) to the inclusion membrane is advantageous for bacterial nutrient acquisition from the host intracellular compartments.

Rab39, a short variant of Rab34, has two isoforms, Rab39a and Rab39b, with 78% identity at the amino acid level (Becker et al., 2009; Chen et al., 2003). Rab39a and Rab39b display different intracellular distribution. Rab39a is associated with late endosomes and lysosomes, and regulates endocytosis, acidification of maturing phagosomes, autophagosome formation and secretion of pro-inflammatory compounds (Becker et al., 2009; Mori et al., 2013; Seto et al., 2011, 2013). In contrast, Rab39b is mainly concentrated at the Golgi complex, and regulates the trafficking to synaptic terminals of glutamate receptors, synaptic transmission, and growth and differentiation of neuronal cells (Giannandrea et al., 2010; Mignogna et al., 2015).

Our work uncovers a new role for the previously uncharacterized Rab39a as a MVB-associated Rab protein that is involved in the targeting of MVBs to chlamydial inclusions. Here, we show that endogenous Rab39a is recruited to chlamydial inclusions. Interestingly, a subset of Rab39a-labelled vesicular structures, likely exosomes delivered by fusion with MVBs, is found within the inclusion lumen. Rab39a is associated with inclusions in different cell types throughout the bacterial developmental life cycle, and this association is mediated by a bacteria-driven process. Rab39a redistribution to chlamydial inclusion surroundings is highly dynamic and depends on its GTP- or GDP-binding state. Nocodazole treatment disrupts Rab39a-mediated trafficking, indicating that microtubules participate in this process. Furthermore, our results indicate that Rab39a is involved in the MVB–inclusion interaction. Notably, Rab39a promotes the delivery of both MVBs and sphingolipids to the growing inclusions. Our findings establish that Rab39a-controlled transport plays a role in inclusion development and chlamydial replication, therefore favouring the intracellular growth of this highly adapted human pathogen.

RESULTS

Rab39a localization to chlamydial inclusions

C. trachomatis, as for many other intracellular pathogens, have developed different strategies to survive and replicate within infected cells. By recruiting certain Rabs and excluding others, these bacteria avoid degradation in the phagocytic pathway and intercept vesicles carrying host molecules required for bacterial growth (Damiani et al., 2014; Gutierrez, 2013). Although several researchers have explored the participation of Rabs in chlamydial infection, this issue is far from being fully understood.

In this study, we analysed the role of Rab39a, a poorly characterized small GTPase, in the intracellular development of *C. trachomatis* serovar L2. In uninfected HeLa cells, endogenous Rab39a displayed a punctate pattern throughout the cytosol, resembling that of small endosomes (Fig. 1A, left panels). Interestingly, there was an evident redistribution of endogenous Rab39a upon *C. trachomatis* infection, with it being re-localized to the chlamydial inclusion periphery (Fig. 1A, right panels). Endogenous Rab39a clearly associated with mid-stage inclusions in almost every cell. Furthermore, images suggest an apparent increment in the amount of Rab39a protein upon

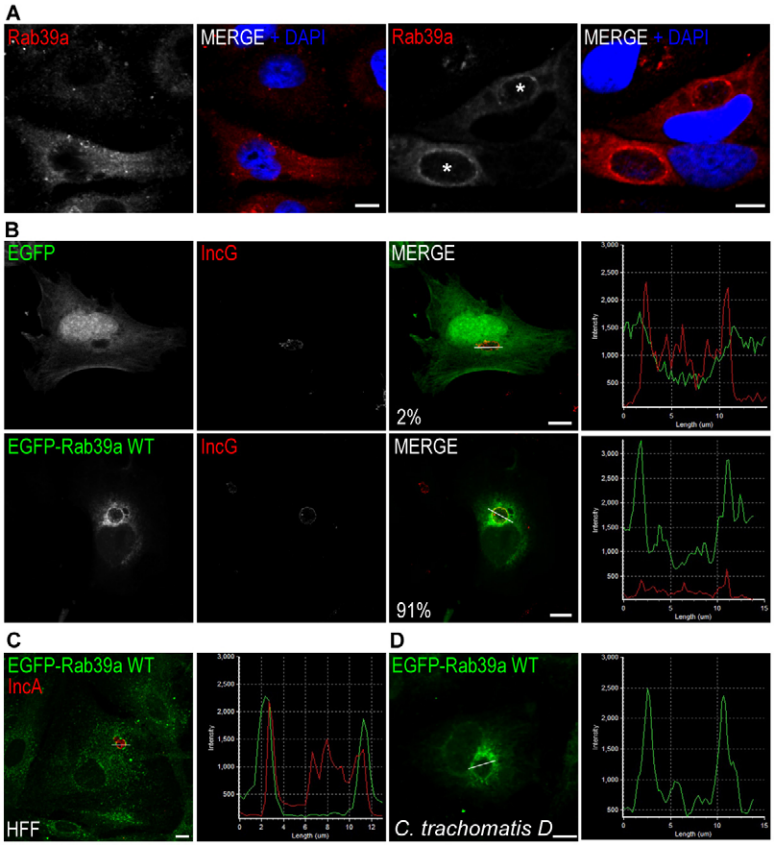

Fig. 1. Rab39a is recruited to the inclusion of *Chlamydia trachomatis*. (A) Uninfected HeLa cells (left panels) and cells infected with *C. trachomatis* serovar L2 (MOI 1) for 24 h (right panels). Endogenous Rab39a was detected using rabbit anti-Rab39a followed by goat Cy3-labelled anti-rabbit-IgG (red) antibodies. DNA was stained with DAPI (blue). Asterisks show the inclusions. Images are representative of two independent experiments. (B) HeLa cells overexpressing EGFP or EGFP–Rab39a-WT (green) were infected with *C. trachomatis* L2 (MOI 1) for 18 h. Inclusion membrane was labelled with polyclonal rabbit anti-IncG followed by goat Cy3-labelled anti-rabbit-IgG (red) antibodies. Right panels show the intensity profiles scanned along the line crossing the inclusion. The red peaks correspond to the bacterial protein IncG and the green peaks indicate EGFP–Rab39a. The percentage of cells in which EGFP or EGFP–Rab39a were found flanking the inclusions during the analysis of the intensity profiles is indicated at the bottom of the corresponding panels. The data are representative of three independent experiments, with 180 cells of each condition analysed (P<0.01, Student's t-test). (C) HFF cells overexpressing EGFP–Rab39a-WT (green) were infected with *C. trachomatis* serovar L2 (MOI 1) for 18 h. Bacterial IncA was immunodetected with polyclonal rabbit anti-IncA followed by goat Cy3-labelled anti-rabbit-IgG (red) antibodies. The right panel shows the intensity profile scanned along the line crossing the inclusion. (D) HeLa cells overexpressing EGFP–Rab39a-WT (green) were infected with *C. trachomatis* serovar D (MOI 1) for 18 h. The right panel shows the intensity profile scanned along the line crossing the inclusion. The green peaks show EGFP–Rab39a surrounding the inclusion developed by *C. trachomatis* serovar D. Scale bars: 10 µm.

Journal of Cell Science (2015) 128, 3068-3081 doi:10.1242/jcs.170092

infection. Hence, we analysed the expression of endogenous Rab39a in HeLa cells infected with *C. trachomatis* at different hours post infection (hpi). Our results show that eukaryotic Rab39a expression did not significantly change upon bacterial infection (supplementary material Fig. S1A). Detection of endogenous Rabs at chlamydial inclusion borders is a difficult task, which has been only accomplished for Rab14 (Capmany and Damiani, 2010). We next examined the intracellular localization of EGFP–Rab39a in infected cells in which inclusions were detected by immunostaining against the bacterial protein IncG (Fig. 1B, lower panels). Similar to the endogenous protein, EGFP–Rab39a concentrated around inclusions in almost every infected cell (91.2%±1.2, mean±s.e.m., n=180, P<0.01, from three independent experiments). The localization of fluorescent proteins was analysed by generating a profile of the intensity distribution of each constituent along a line traversing the chlamydial inclusions. EGFP–Rab39a (Fig. 1B, green line) was found flanking mid-stage inclusions where the bacteria (Fig. 1B, red line) were confined.

To determine whether the association of Rab39a with *C. trachomatis* inclusions occurs in other cell types, we examined EGFP–Rab39a localization in infected HFF cells, a human foreskin fibroblast cell line, and in CHO cells, a Chinese hamster ovary cell line. Similar to the results obtained in HeLa cells, EGFP–Rab39a was found surrounding chlamydial inclusions in both of these cell types (Fig. 1C; and data not shown). Next, we examined the intracellular distribution of this GTPase in HeLa cells infected with *C. trachomatis* serovar D to assess whether Rab39a association with inclusions depends on *Chlamydia* serovar. Likewise, images and intensity profiles showed that EGFP–Rab39a was concentrated around mid-stage inclusions (Fig. 1D). Taken together, our findings suggest that both endogenous and overexpressed Rab39a are recruited to chlamydial inclusions.

Characterization of Rab39a recruitment to chlamydial inclusions

C. trachomatis gene expression varies throughout development, thus, inclusions might display different features throughout time. To test this possibility, we analysed the intracellular localization of EGFP–Rab39a in HeLa cells infected with *C. trachomatis* for different periods of time. Representative images and the percentage of cells displaying a similar pattern are indicated at the bottom of each panel in Fig. 2A. At early stages (4 hpi), multiple non-fused chlamydial vacuoles that were trafficked to the perinucleus began to accumulate EGFP–Rab39a. At mid-cycle (8 hpi to 12 hpi), EGFP–Rab39a was concentrated around the clustered inclusions at the perinuclear region of infected cells. By 18 hpi, the EGFP–Rab39a association with the single large perinuclear inclusion was much more prominent. Furthermore, EGFP–Rab39a remained associated with the inclusions throughout the entire chlamydial developmental cycle. Interestingly, at later stages of infection (32–48 hpi), several EGFP–Rab39a-labelled small vesicles appeared to locate inside inclusions in more than half of the cells analysed (Fig. 2A, lower right panels). To determine whether these vesicles are within the inclusion lumen, we stained the bacterial and eukaryotic DNA with Hoechst 33342 (blue) and assessed the subcellular localization of Rab39a-labelled structures by three-dimensional (3D) fluorescence microscopy. A series of z-optical sections were taken through the entire thickness of the cell for a 3D-reconstruction, in which we observed EGFP–Rab39a labelled vesicles (green) close to the bacteria (blue). A single x-y section of the cell is shown in Fig. 2B, and x-z and y-z projections are on the bottom and on the right side of the merged panel, respectively. Images show some EGFP–Rab39-labelled vesicles inside late-stage inclusions (black arrowheads), often adjacent to bacteria (white arrowhead). In cells infected for 32 h, we observed the presence of at least one EGFP–Rab39a-labelled vesicle inside inclusions in the majority of the cells (72%, n=60).

Next, we assessed the association of Rab39a with inclusions using spinning-disk microscopy in living cells to avoid fixation artefacts. Live-cell imaging revealed a highly dynamic vesicular trafficking between EGFP–Rab39a-positive compartments and the inclusions at different stages of chlamydial development. For these experiments, HeLa cells were infected for different periods of time with *C. trachomatis* transformed strains overexpressing mCherry protein (red) (Agaisse and Derré, 2013). Interestingly, small EGFP–Rab39a-positive vesicles move forward and backward near the chlamydial inclusions, suggesting fusion and fission events between Rab39a-positive structures and the inclusions (Fig. 2C; supplementary material Movie 1).

A series of experiments was performed to assess the involvement of bacterial proteins in the recruitment of Rab39a to chlamydial inclusions. HeLa cells overexpressing EGFP–Rab39a (green) were incubated with living or heat-killed *C. trachomatis* detected with anti-elementary-body antibodies (red). DAPI staining labelled bacteria and the host cell nuclei (blue). Images show that EGFP–Rab39a did not associate with dead bacteria (supplementary material Fig. S1B). Furthermore, EGFP–Rab39a failed to localize to chlamydial inclusions in the presence of chloramphenicol, a bacterial translation inhibitor, but resumed upon removal of the antibiotic (supplementary material Fig. S1C; data not shown). These data suggest that *C. trachomatis*-mediated remodelling of the inclusion is necessary for recruitment of Rab39a.

To determine the specificity of the interaction between Rab39a and chlamydial inclusions, HeLa cells overexpressing different Rab GTPases were infected with *C. trachomatis* for 24 h. Cells were processed for immunofluorescence with anti-IncA antibodies. Consistent with previous data (Rzomp et al., 2003; Scidmore et al., 2003), although adjacent to the inclusions, Rab5 (see Fig. 4Bf–h) and EGFP–Rab7a (Fig. 3A, upper panels) did not associate with the inclusions. In contrast, this is the first report showing that the endocytic and lysosomal Rab34 (Fig. 3A, second row), whose short variant is Rab39, and Rab39b (Fig. 3A, lower panels), an isoform that functions at the ER–Golgi were recruited to the chlamydial inclusions interface. The percentage of cells in which Rabs were found to be associated with the inclusions is indicated in each case.

Next, we investigated whether Rab39a association with the inclusions depends on its GTP- or GDP-binding state by overexpression of the constitutively active GTP-bound (EGFP–Rab39a-Q72L) or the inactive GDP-bound (EGFP–Rab39a-S22N) Rab39a mutant proteins. Images and intensity distribution profiles show that wild-type (WT) Rab39a and Rab39a Q72L, but not Rab39a S22N, localized at chlamydial inclusions (shown by IncA-labelling) (Fig. 3B), indicating that Rab39a is recruited to the chlamydial inclusions in a guanine-nucleotide-dependent manner. Distribution intensity profiles of 50 cells for each condition were analysed to calculate the percentage of cells depicting positive recruitment of each GFP to the boundaries of the inclusions. In agreement with these findings, mutants of Rab4, Rab6, Rab11 and Rab14 only able to bind GDP do not associate with chlamydial inclusions (Capmany and Damiani, 2010; Moorhead et al., 2007; Rzomp et al., 2006).

Both, chlamydial inclusion migration to the perinucleus and homotypic fusion are dependent on an intact microtubule network (Grieshaber et al., 2003; Richards et al., 2013). Furthermore, it has been recently demonstrated that microtubule depolymerization

Journal of Cell Science

Journal of Cell Science (2015) 128, 3068-3081 doi:10.1242/jcs.170092

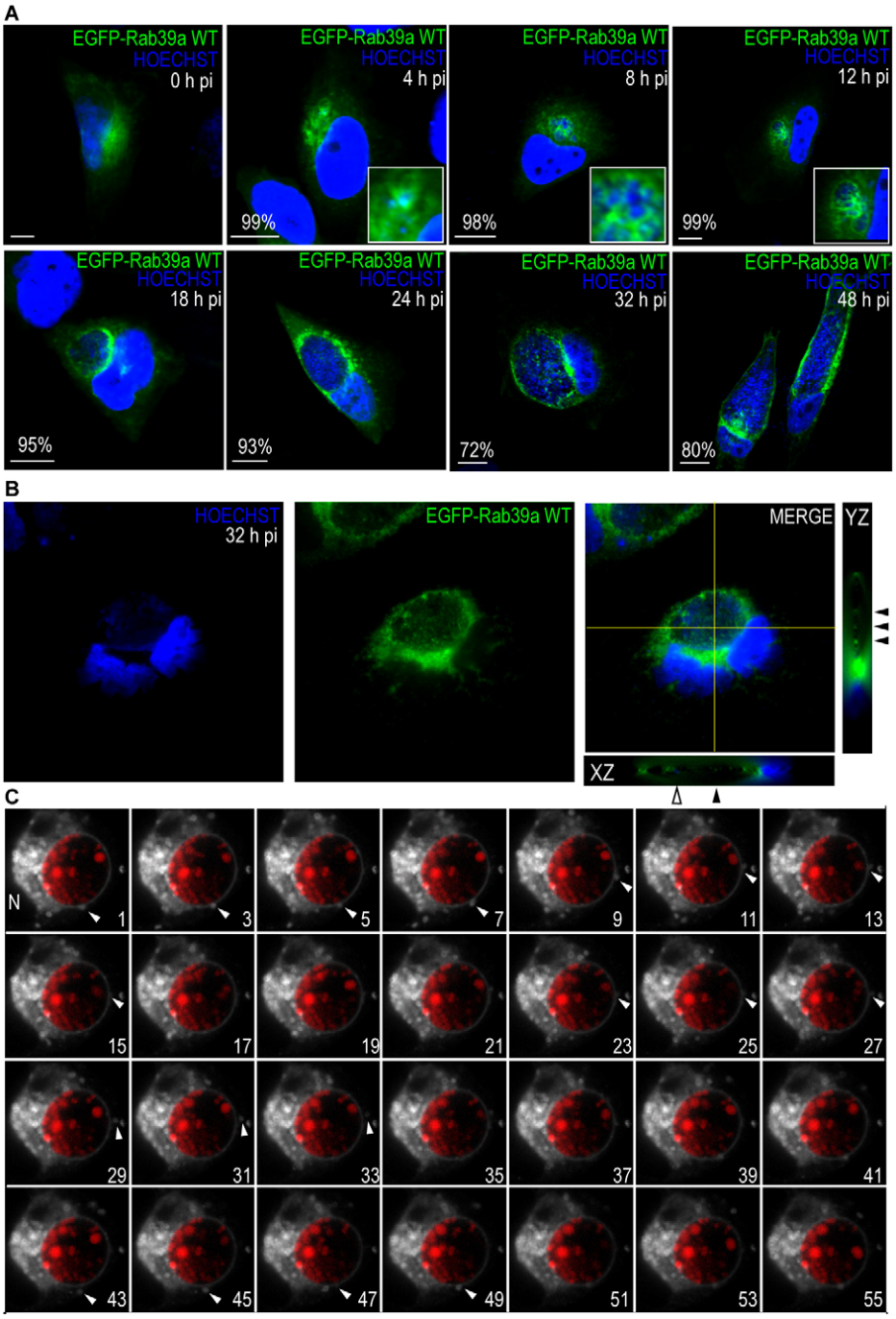

Fig. 2. Rab39a associates with chlamydial inclusions throughout the developmental cycle. (A) HeLa cells transiently overexpressing EGFP–Rab39a-WT (green) were infected with *C. trachomatis* serovar L2 at an MOI of 25 (for 4 h to 12 h assays) and of 5 (for 18 h to 48 h assays). At the indicated post infection times (hpi), cells were fixed and stained with Hoechst 33342, which labels bacterial and eukaryotic DNA (blue). Insets show a magnification of the perinuclear region of infected cells at early stages of chlamydial inclusion development. Scale bars: 10 µm. Images are representative of two independent experiments. The percentage of cells with similar patterns is indicated at the bottom of the panels. (B) A single *x-y* section from the stack of images of a cell infected for 32 h, and *x-z* and *y-z* projections on the bottom and left side of the right panel, respectively. In the projections, black arrowheads point to the Rab39a-labelled vesicles that are inside the inclusion next to the bacteria, which is indicated by an open arrowhead. (C) HeLa cells transiently overexpressing EGFP–Rab39a were infected with *C. trachomatis* transformed strains harbouring p2TK2-SW2 IncDProm-mCherry-IncDTerm (mCherry) for 24 h. Insets show a magnification of the inclusion area. Numbered panels show a gallery of time-lapse images acquired every 2 s by spinning disk microscopy (from supplementary material Movie 1). The nucleus of the cell is indicated with N. White arrowheads point to a Rab39a-positive vesicles coming and detaching from the inclusion.

reduces inclusion growth and chlamydial replication in cells treated with nocodazole for long periods of time (Al-Zeer et al., 2014). Live-cell imaging showed EGFP–Rab39a-positive vesicles moving along straight lines, likely microtubules (supplementary material Movie 1). Therefore, we analysed the effect of nocodazole, a microtubule-destabilizing drug, on uninfected and *C.-trachomatis*-infected cells. Time-lapse video microscopy shows that the movement of Rab39a-positive vesicles in uninfected cells was drastically reduced after a short-term treatment with nocodazole (10 µM, 1 h) (supplementary material Movie 2, right panel). Consistent with this, Rab39a-positive vesicle movement was almost suppressed in *C.-trachomatis*-infected cells after nocodazole treatment (supplementary material Movie 3, right panel). Crucially, we found that altering microtubule integrity impaired Rab39a recruitment to the chlamydial inclusions (Fig. 3C, white arrowheads). Depolymerization of the microtubular network was confirmed by tubulin staining. Collectively, live-cell imaging and confocal microscopy suggest that *C. trachomatis* modify the inclusion early during the developmental cycle to recruit Rab39a, and that Rab39a association with inclusions is GTP-dependent and involves dynamic microtubules.

Rab39a colocalizes with CD63 and LBPA in *C. trachomatis*-infected cells

To understand the implications of Rab39a recruitment to chlamydial inclusion development, we examined the subcellular distribution of this GTPase in both uninfected (Fig. 4A) and *C. trachomatis*-infected (Fig. 4B) HeLa cells. Intracellular distribution of EGFP–Rab39a in uninfected cells is more extensively displayed in supplementary

Journal of Cell Science (2015) 128, 3068-3081 doi:10.1242/jcs.170092

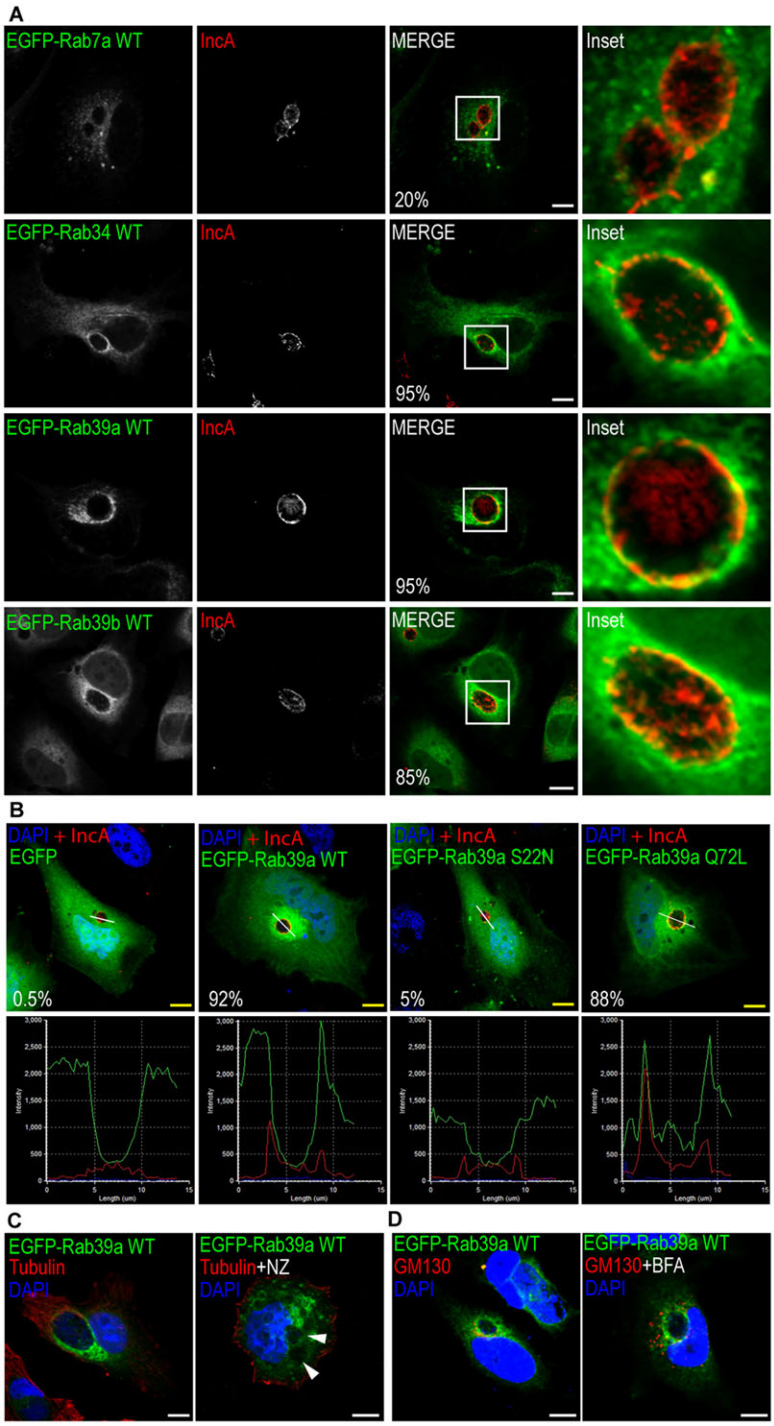

Fig. 3. Characterization of Rab39a recruitment to chlamydial inclusions. (A) HeLa cells were transiently transfected with pEGFP-Rab7a WT (upper panels), pEGFP-Rab34 WT (upper middle panels), pEGFP-Rab39a WT (lower middle panels) or pEGFP-Rab39b (lower panels), and 24 h later, cells were infected with *C. trachomatis* serovar L2 (MOI 1) for 24 h. Inclusion membrane and bacteria were immunodetected with polyclonal rabbit anti-IncA followed by goat Cy3-labelled anti-rabbit-IgG (red) antibodies. Insets show a magnification of the selected areas. The percentage of cells in which the corresponding Rab is found associated with the inclusion borders, as assessed by analysis of distribution intensity profiles (40 cells of each condition were analysed from three independent experiments) are shown at the bottom of the panels. (B) HeLa cells transiently transfected with pEGFP, pEGFP-Rab39a WT, pEGFP-Rab39a S22N (GDP-bound form) or pEGFP-Rab39a Q72L (GTP-bound form) were infected with *C. trachomatis* serovar L2 (MOI 1) for 18 h and analysed by confocal microscopy. Inclusion membrane and bacteria were immunodetected with polyclonal rabbit anti-IncA followed by goat Cy3-labelled anti-rabbit-IgG (red) antibodies. DNA was stained with DAPI (blue). Lower panels show the intensity profiles scanned along the line crossing the inclusion. The percentage of cells in which the indicated proteins were found flanking the inclusions in the analysis of the intensity profiles are displayed at the bottom of the panels. Data were obtained from two independent experiments (50 profiles of each condition were analysed). (C,D) HeLa cells were transfected with pEGFP-Rab39a WT (green) and 24 h later were infected with *C. trachomatis* serovar L2 (MOI 5). After the internalization period (2 h), cells were washed to remove non-internalized bacteria and incubated for 1 h with complete medium. Then, (C) nocodazole (NZ, 2 µM) or (D) brefeldin A (BFA, 1 µg/ml) was added, and finally, cells were fixed at 18 hpi. White arrowheads indicate chlamydial inclusions. Tubulin and the Golgi marker GM130 were detected using specific monoclonal mouse antibodies followed by goat Cy3-labelled anti-mouse-IgG (red) antibody. DNA was labelled with DAPI (blue). Scale bars: 10 µm.

material Fig. S2. Colocalization assays of EGFP–Rab39a with well-characterized markers of the Golgi complex and endocytic organelles were performed first in uninfected cells and then in cells infected with *C. trachomatis* for 18 h. Pearson correlation coefficients (*r*) were calculated and are indicated at the bottom of the panels in Fig. 4B. Interestingly, images show that EGFP–Rab39a did not localize to the Golgi complexes – labelled with anti-TGN46 (also known as TGOLN2) or with anti-GM130 antibodies – in uninfected or infected cells (Fig. 3D; Fig. 4Aa,Bb–d). Consistent with this, Rab39a association with chlamydial inclusions was not affected by brefeldin A (BFA) treatment (Fig. 3D, right panel). Early endosomes, identified with anti-Rab5 antibodies, localized at the cell periphery and displayed little overlap with EGFP–Rab39a (Fig. 4Ae,Bf–h). Similar results were obtained by loading early endosomes with Texas-Red-conjugated dextran (data not shown). By contrast, EGFP–Rab39a displayed a high degree of colocalization with LysoTracker (a marker of acidic compartments) (Fig. 4Ai,Bj–l) and lysosome-associated membrane protein 1 (LAMP1) (Fig. 4Am,Bn–p), not only in uninfected cells but also at the vicinity of the chlamydial inclusions. Surprisingly, there was little colocalization between EGFP–Rab39a and cathepsin D in either condition (Fig. 4Aq,Br–t), indicating that Rab39a labels a subset of vesicles from the late endocytic pathway that are devoid of cathepsin D. In agreement with our findings, it has been reported that Rab39a regulates

Journal of Cell Science (2015) 128, 3068-3081 doi:10.1242/jcs.170092

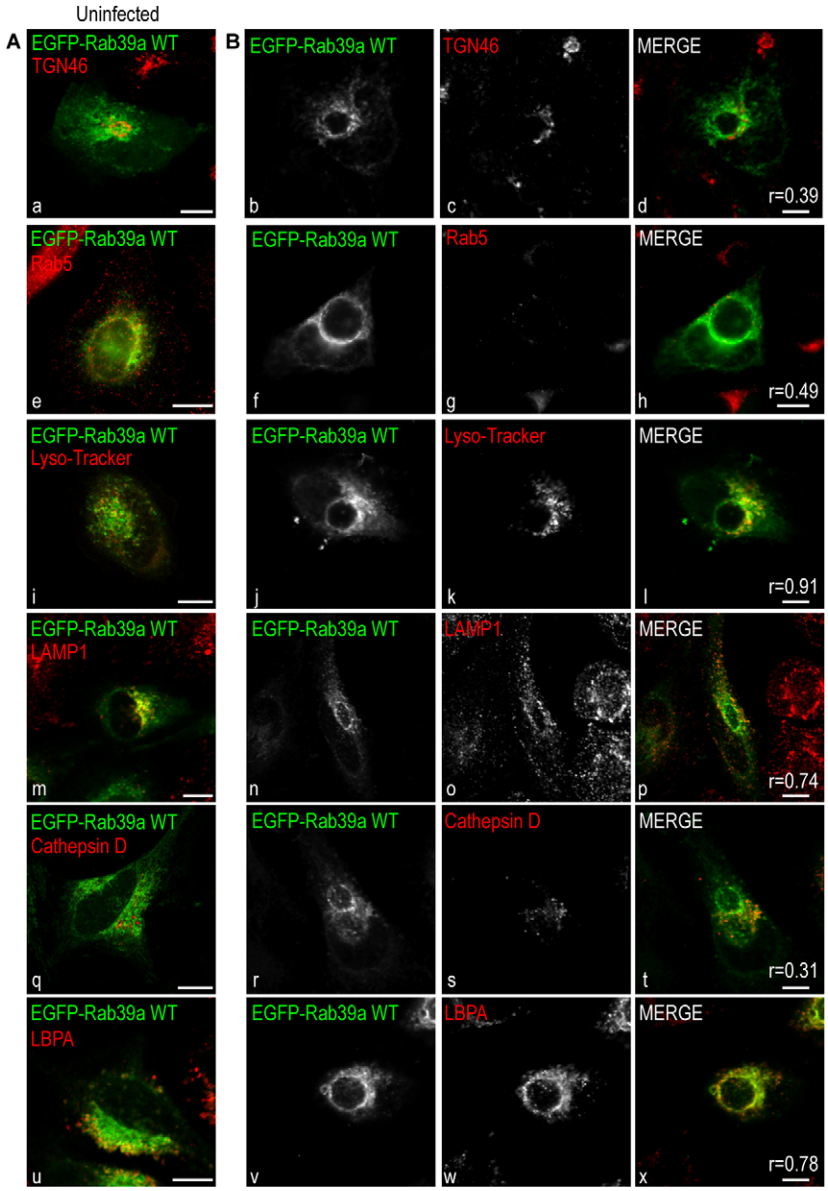

Fig. 4. Rab39a localizes at the late endocytic pathway. HeLa cells transiently overexpressing EGFP–Rab39a (green), (A) uninfected or (B) infected with *C. trachomatis* serovar L2 (MOI 1) for 18 h, were stained with markers of different subcellular structures: TGN46 (for the trans-Golgi network, a–d), Rab5 (for early endosomes, e–h), LysoTracker (for acidic compartments, i–l), LAMP1 (for late endosomes and lysosomes, m–p), cathepsin D (for hydrolytic enzymes, q–t) and LBPA (for multivesicular bodies, u–x). Cells were incubated with LysoTracker (red) for 10 min prior to fixation or were inmunolabelled with the appropriate primary antibodies followed by goat Cy3-labelled anti-mouse-IgG (red) antibody, as indicated. Scale bars: 10 µm. Images are representative of three independent experiments. Pearson's colocalization coefficients (*r*) between Rab39a and the different organelle markers are shown at the bottom of the right panels (data are from three independent experiments in which 50 cells of each group were analysed).

phagosomal acidification, but not cathepsin D recruitment, to *Mycobacterium tuberculosis*-containing phagosomes (Seto et al., 2011).

To further characterize the nature of Rab39a-positive subcellular structures, we analysed their localization in conjunction with that of markers for MVBs, which are late endocytic organelles enriched in LBPA. Interestingly, there was a high degree of colocalization between EGFP–Rab39a (green) and LBPA (red) in both, uninfected and infected cells (Fig. 4Au,Bv–x). In addition, MVBs were also identified by labelling the tetraspanin CD63 (red), and it was found that this marker showed almost complete colocalization with EGFP–Rab39a (green) in *C. trachomatis*-infected cells, as shown in Fig. 5A [the Pearson correlation coefficient (*r*) is indicated at the bottom of the right panel]. Furthermore, vesicles dually labelled with Rab39a and CD63 were clearly detected within the lumen and surrounding the inclusions (Fig. 5A, inset). A 3D image built with the *z*-slices of the cell is shown in supplementary material Movie 4, in which Rab39a and CD63 double-positive small vesicles can be observed inside the inclusion that it is delimited by Rab39a association to its borders.

To more accurately assess the interaction between MVBs and chlamydial inclusions, we performed ultra-structural analysis of infected cells. EGFP–Rab39a-overexpressing cells were first infected with *C. trachomatis* for 24 h. Then, the nature of the vesicles observed within the inclusion lumen as well as in the vicinity of the inclusions was further analysed by immunodetecting CD63. Electron microscopy images show vesicular structures dually labelled with Rab39a and CD63, confirming their identity as MVBs (Fig. 5Ba,b; supplementary material Fig. S3a, black arrows). Several MVBs are in close contact with the chlamydial inclusion membrane, suggesting tight interaction and fusion events between both structures (Fig. 5Ba,b; supplementary material Fig. S3a, black arrowheads). Furthermore, both the proteins EGFP–Rab39a and CD63 were found to be associated with vesicular structures that were adjacent to bacteria, which might be delivered to the lumen of chlamydial inclusions by fusion with Rab39a-positive MVBs (Fig. 5Ba,b, open arrowheads). Several bacteria are indicated with asterisks. In addition, Rab39a was found within the lumen and was associated with the inclusion membrane (Fig. 5Bb, white arrows). In another experiment,

Journal of Cell Science (2015) 128, 3068-3081 doi:10.1242/jcs.170092

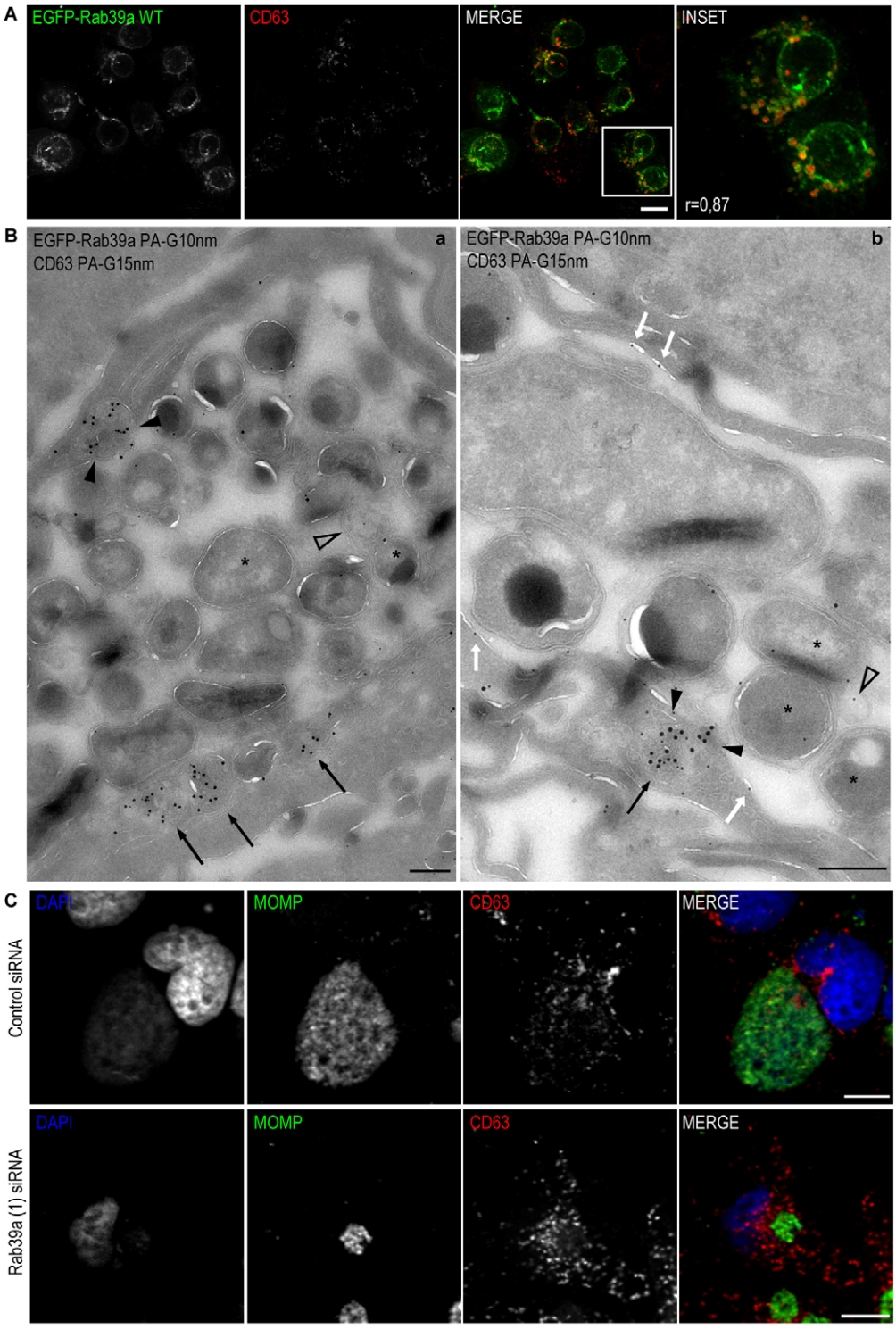

Fig. 5. Rab39a localizes at multivesicular bodies and mediates their transport to chlamydial inclusions. (A) HeLa cells transiently overexpressing EGFP–Rab39a-WT (green) were infected with *C. trachomatis* serovar L2 (MOI 1) for 24 h and stained with mouse anti-CD63 antibodies followed by goat Cy3-labelled anti-mouse-IgG antibodies (red). The inset shows a magnification of the selected area. Scale bar: 10 µm. (B) Ultrathincryosections (a,b) of *C. trachomatis*-infected cells (MOI 1, 24 h) were double immunogold labelled for CD63 (PA-G15) and Rab39a (PA-G10). Several multivesicular bodies (MVBs) labelled for CD63 and Rab39a were closely apposed to the limiting membrane of the chlamydial inclusion (black arrows). Note CD63 and Rab39a double-positive MVBs that were probably undergoing fusion with the chlamydial inclusion at the time of fixation (black arrowheads). Small vesicular structures, dually labelled with CD63 and Rab39a, were found within inclusion lumen in close contact with bacteria (open arrowheads). Several bacteria are highlighted with asterisks. Rab39a was found to be associated with the chlamydial inclusion membrane (b, white arrows). Scale bars: 200 nm. (C) HeLa cells were transfected with control siRNA or specific Rab39a (1) siRNA and infected with *C. trachomatis* L2 (MOI of 5) at 48 h post transfection. Then, cells were fixed at 24 hpi and bacteria were labelled with FITC-coupled anti-MOMP antibodies (green) and MVBs with mouse monoclonal anti-CD63 followed by goat Cy3-labelled anti-mouse-IgG antibodies (red). DAPI stained eukaryotic and bacterial DNA (blue). Scale bars: 10 µm. Images are representative of three independent experiments. Note the decrease in the amount of CD63 labelling within inclusion lumen in Rab39a-depleted cells (lower panels).

EGFP–Rab39a-overexpressing cells infected with *C. trachomatis* [multiplicity of infection (MOI) 1, 24 h] were allowed to internalize bovine serum albumin (BSA)–gold conjugates for 60 min. Internalized BSA accumulated in vesicular compartments morphologically identified as MVBs, which were also labelled with EGFP–Rab39a. BSA was transported to and incorporated into chlamydial inclusions confirming interaction with the late endocytic pathway (supplementary material Fig. S3b, white arrowheads). Rab39a was found to be associated with the inclusion membrane as well as within the inclusion lumen (supplementary material Fig. S3b, white arrows). These findings imply that the arrival and incorporation into the inclusions of molecules internalized by endocytosis is mediated through selective sorting and delivery of a subset of late endocytic organelles, likely MVBs, and that this process involves a Rab39a-mediated trafficking pathway.

Rab39a is involved in the transport of MVBs and sphingolipids to the inclusions

The participation of Rab39a in the transport of MVBs to chlamydial inclusions was further analysed using loss-of-function approaches.

Journal of Cell Science (2015) 128, 3068-3081 doi:10.1242/jcs.170092

HeLa cells were transfected with small interfering RNAs (siRNAs) against luciferase (control cells) or with specifically designed siRNA against Rab39a [Rab39a (1) siRNA]. At 48 h post-transfection, control and Rab39a-depleted cells were infected with *C. trachomatis* for 24 h. MVBs were labelled with anti-CD63 antibodies (red), bacteria with anti-MOMP antibodies (green) and DNA with DAPI (blue). Noticeably, the localization of CD63 at chlamydial inclusions decreased when Rab39a expression was knocked down (Fig. 5C, lower panels). These results indicate that Rab39a might accomplish a role in the re-routing of MVBs to the chlamydial inclusions.

MVBs are a major source of lipids for growing inclusions. Therefore, we investigated whether Rab39a is involved in sphingolipid delivery from these organelles to the inclusions. HeLa cells overexpressing EGFP (control), EGFP–Rab39a-WT, EGFP–Rab39a-S22N or EGFP–Rab39a-Q72L were infected with *C. trachomatis* for 18 h. Before fixation, cells were incubated with BODIPY-Tr-Ceramide (red), a fluorescently labelled precursor usually used to analyse transport of endogenously synthesized sphingomyelin to the inclusions. Interestingly, a high degree of colocalization between EGFP–Rab39a-WT and sphingolipids was observed at the chlamydial inclusion membrane and in vesicles nearby (Fig. 6A, see insets). The right panels of Fig. 6A show distribution intensity profiles of EGFP-tagged proteins (green line) and sphingolipids (red line) along a line traversing the chlamydial inclusions. Cells overexpressing EGFP–Rab39a-WT or its active GTP-bound mutant (EGFP–Rab39a-Q72L) showed a significantly increase in the amount of sphingolipids accumulated within the inclusions compared to control or the cells overexpressing inactive mutant, as assessed by measuring the intensity of red fluorescence associated with inclusions by confocal microscopy (Fig. 6B). These results point to a role for Rab39a in sphingolipid transport to chlamydial inclusions.

We confirmed the participation of Rab39a in the delivery of host sphingolipids to the inclusions by RNA interference loss-of-function assays. HeLa cells were transfected with siRNAs against luciferase (control cells) or with specifically designed siRNA against Rab39a

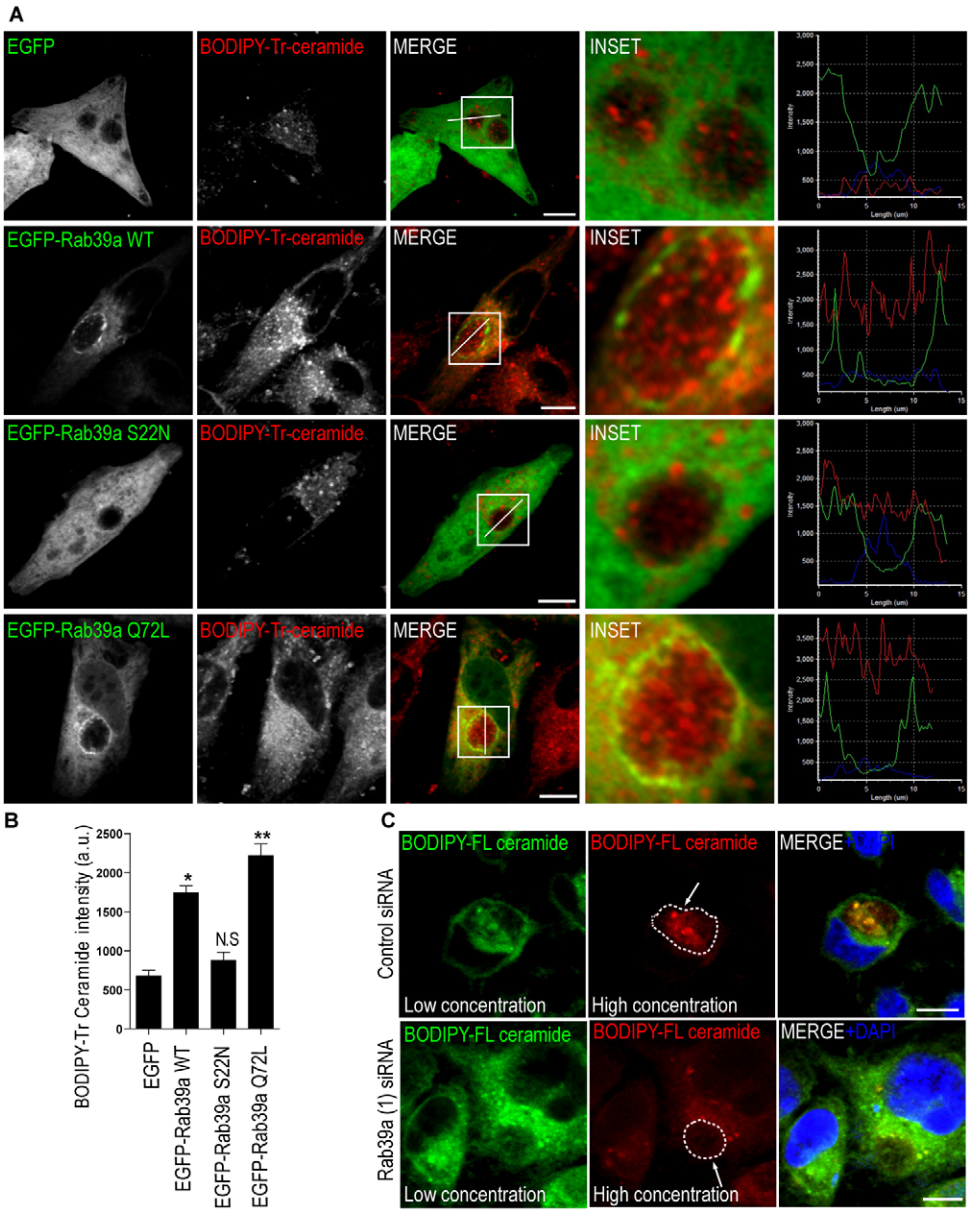

Fig. 6. Rab39a regulates the delivery of sphingolipids to chlamydial inclusions. (A) HeLa cells overexpressing EGFP, EGFP–Rab39a-WT, EGFP–Rab39a-S22N or EGFP–Rab39a-Q72L (green) were infected with *C. trachomatis* serovar L2 (MOI 5) for 18 h. Before fixation, cells were incubated 30 min with 5 µM BODIPY-Tr-Ceramide (red) and chased for 30 min. Insets show a magnification of a chlamydial inclusion. Right panels show the intensity distribution profiles scanned along a line crossing the inclusion. (B) Bar graph representing the fluorescence intensity of the red labelling (sphingolipids) inside the inclusions, as quantified by confocal microscopy and expressed as arbitrary units. Data were obtained from three independent experiments (n=40, $^{**}P$<0.001, one-way ANOVA and Bonferroni's multiple comparison test). (C) HeLa cells were transfected with control siRNA or Rab39a (1) siRNA for 48 h. Then cells were infected with *C. trachomatis* L2 (MOI of 5) and fixed at 24 hpi. Before fixation, cells were incubated for 30 min with a different lipid probe, BODIPY-FL-Ceramide, and chased for 30 min. At high concentrations BODIPY-FL-Ceramide exhibits red fluorescence whereas in low concentration this ceramide displays green fluorescence. DNA was labelled with DAPI (blue). Dotted lines delimit the inclusions that are highlighted by the arrows. Scale bars: 10 µm.

Journal of Cell Science (2015) 128, 3068-3081 doi:10.1242/jcs.170092

[Rab39a (1) siRNA]. At 48 h post-transfection, cells were infected with *C. trachomatis* for 24 h. Before fixation, cells were incubated for 30 min with ceramide coupled to a different fluorescent compound (BODIPY-FL-Ceramide). In this latter case, sphingolipids exhibit red fluorescence at high concentrations, whereas at low concentrations they display green fluorescence. Images confirm the sphingolipid accumulation within inclusions of control cells (denoted by the red fluorescence inside inclusions; Fig. 6C, upper panels). By contrast, the amount of sphingolipids within chlamydial inclusions was significantly reduced in Rab39a-depleted cells, which only displayed weak green fluorescence at the inclusion area (Fig. 6C, lower panels). Taken together, these data indicate that Rab39a controls the transport of sphingolipids to the developing chlamydial inclusions.

Rab39a promotes inclusion development and chlamydial replication

C. trachomatis-driven recruitment of Rab39a to the inclusions, and the participation of this Rab in sphingolipid delivery to the growing inclusions suggest that this GTPase plays a role during infection development. To address whether this was the case, HeLa cells were depleted of endogenous Rab39a using specifically designed siRNA (as indicated in the section above). Rab39a depletion (69%) was confirmed by western blotting (Fig. 7B). At 48 h post transfection, cells were infected with *C. trachomatis* for an additional 48 h. Then, cells were lysed to collect the bacterial progeny. The harvested infectious particles were titrated, in serial dilutions, on HeLa cells. At 24 hpi, inclusions were labelled with anti-MOMP (an IgG that recognizes the major outer membrane protein present in every developmental form of *C. trachomatis*) and anti-elementary-body (an IgG that only identifies elementary bodies) antibodies. Images show that fewer inclusions were generated when the progeny collected from Rab39a-depleted cells was assayed (Fig. 7A, lower panels). The yield of infectious bacteria was quantified by determining the number of inclusion-forming units (IFUs). Silencing of Rab39a reduced the number of infectious progeny (Fig. 7C). Similarly, silencing of distinct Rabs (Rab6, Rab11 and Rab14) reduces but does not suppress bacterial replication and infectivity (Capmany and Damiani, 2010; Rejman Lipinski et al., 2009). Next, two siRNA against Rab39a; Rab39a (1) siRNA or Rab39a (3) siRNA and a combination of both siRNAs (1 and 3) were used to transfect cells. Rab39a depletion was assessed by western blotting (Fig. 7D,E). In this set of experiments, at 48 h post-transfection with siRNA, cells were infected with *C. trachomatis* for 24 h. Inclusions were detected with anti-MOMP antibodies and the inclusion size area was measured by confocal microscopy. Our results show that fewer and smaller inclusions were developed in Rab39a-depleted cells (Fig. 7F). Thus, Rab39a-depleted cells are less efficient in the generation of a productive infection, suggesting a failure in chlamydial replication and/or in the generation of infectious bacteria.

The participation of Rab39a on chlamydial replication was further confirmed in HeLa cells overexpressing EGFP (control), EGFP–Rab39a-WT, EGFP–Rab39a-Q72L or EGFP–Rab39a-S22N. Cells were infected for 48 h, and then lysed, and the yield of infectious particles was titrated on HeLa cells. Bacteria were labelled with anti-MOMP (green) and anti-elementary-body (red) antibodies. The progenies collected from Rab39aWT or its active GTP-bound mutant overexpressing cells generated more and bigger inclusions compared to control or EGFP–Rab39a-S22N-overexpressing cells (supplementary material Fig. S4A). Accordingly, the numbers of infectious particles recovered from cells overexpressing Rab39a WT or its active GTP-bound mutant increased significantly, as assessed by IFU assays (supplementary material Fig. S4B). The size of the inclusions is shown in the scatter plot graph (supplementary material Fig. S4C). The increase in the yield of infectious particles correlated with the enlargement of inclusion size. In agreement with our observations, previous reports indicate that inclusion growth and development is accelerated in cells infected with high amounts of bacteria (Scidmore et al., 2003).

Taken together, our findings show that the decrease in the yield of infectious particles recovered from Rab39a-depleted cells, as well as, from cells overexpressing the inactive Rab39a GDP-bound mutant, was small but significant, and it was verified in all assays.

Rab39 is a short variant of Rab34, hence this latter GTPase could be acting to overcome the detrimental effect of depletion of Rab39a on *C. trachomatis* replication and infectivity. Images show a high degree of overlap between both Rabs (Fig. 8A). Hence, we analysed the development of chlamydial inclusions in EGFP–Rab34-WT-overexpressing HeLa cells, in Rab39a-depleted cells and in Rab39a-depleted cells that overexpressed EGFP–Rab34-WT. Interestingly, overexpression of Rab34 WT did not overcome the negative impact on chlamydial inclusion growth caused by Rab39a silencing (Fig. 8B). Accordingly, IFU assays showed that the decrease of bacterial progeny caused by Rab39a depletion could not be rescued by overexpression of the closely related Rab34 GTPase (Fig. 8C). Taken together, our results demonstrate that Rab39a is required for an efficient inclusion development and the replication of *C. trachomatis*.

DISCUSSION

Chlamydial inclusions quickly dissociate from the endocytic pathway and avoid fusion with lysosomes (Fields and Hackstadt, 2002). Initial studies failed to identify early endocytic tracers (dextran, transferrin, Lucifer yellow) as well as late endosomal and lysosomal markers (mannose-6-phosphate receptor, cathepsin D, ATPase and lysotracker) at chlamydial inclusions (Heinzen et al., 1996; Scidmore et al., 2003; Taraska et al., 1996). In this work, we show that internalized BSA, which accumulates in vesicular compartments immunodetected and morphologically identified as MVBs by electron microscopy, reaches the lumen of chlamydial inclusions. This indicates the interaction of inclusions with organelles of the endocytic pathway (Fig. 5B; supplementary material Fig. S3). Typical Rabs of the endocytic pathway, like Rab5, Rab7 and Rab9, do not associate with chlamydial inclusions (Scidmore et al., 2003). We confirmed that Rab7, the archetypal marker of late endocytic vesicles, is not recruited to inclusions. By contrast, we show that the late endocytic and lysosomal Rab34 associates with chlamydial inclusions (Fig. 3A). More importantly, endogenous Rab39a protein was detected at the borders of chlamydial inclusions, a task that is difficult to achieve with available antibodies owing to low protein expression (Fig. 1A). Given that we identify Rab39a on late endocytic organelles, this report becomes the first to demonstrate the interaction of inclusions with a Rab that functions in the late endocytic pathway.

Recent reports have demonstrated that MVBs and lysosomes are important for inclusion development and chlamydial replication (Ouellette et al., 2011; Robertson et al., 2009). Despite the high impact of these late endocytic organelles on chlamydial infection outcome, the molecular mechanisms underlying their interaction are largely unknown. We found that Rab39a is associated with late endocytic structures that are strongly labelled with CD63 (Kobayashi et al., 2000), a tetraspanin that identifies MVBs (Fig. 5A,B). Furthermore, our findings show that Rab39a labels a

Journal of Cell Science (2015) 128, 3068-3081 doi:10.1242/jcs.170092

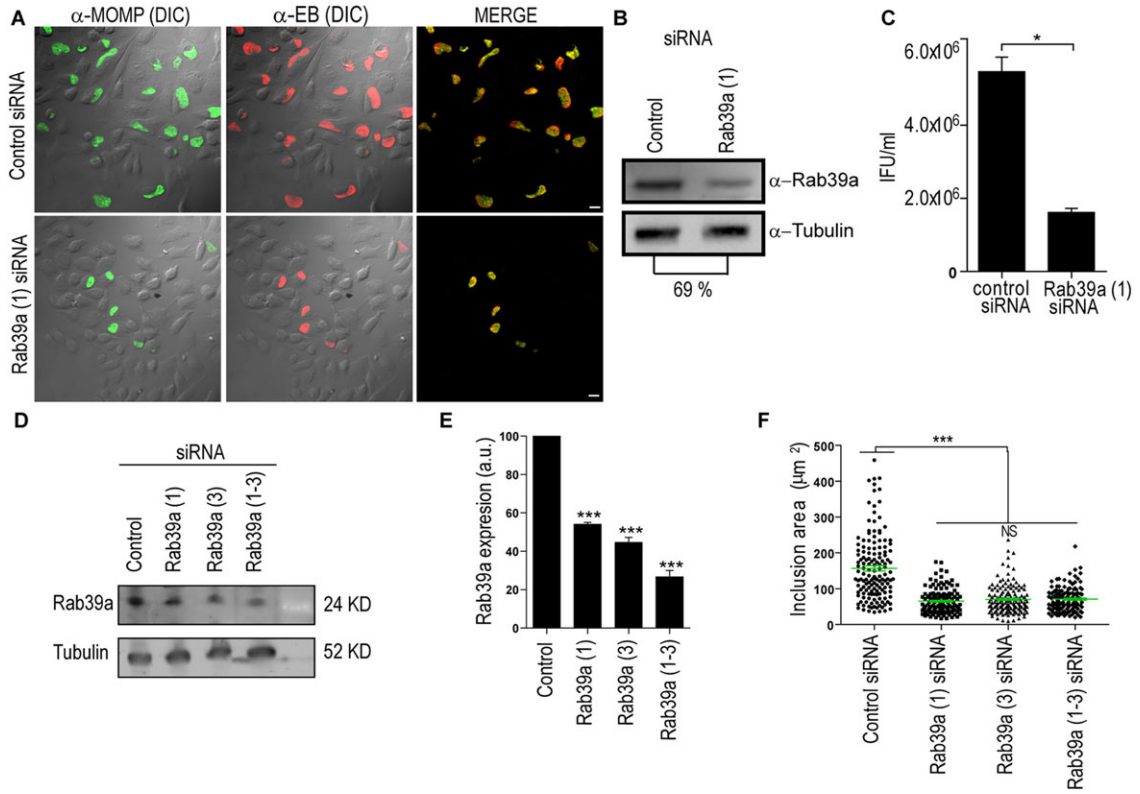

Fig. 7. Rab39a favours bacterial multiplication and inclusion development. HeLa cells were transfected with control siRNA or specific Rab39a (1) siRNA and infected with *C. trachomatis* L2 (MOI of 5) at 48 h post transfection. After 2 days, the infected cells were lysed and the infectious particles (elementary bodies, EB) were titrated, in serial dilution, on HeLa cells. (A) Images show the inclusions developed at 24 h by progenies collected from control (upper panels) and Rab39a-depleted (lower panels) cells. *C. trachomatis* was detected using FITC-coupled anti-MOMP (green) antibody or anti-elementary-body antibodies followed by goat Cy3-labelled anti-mouse-IgG (red) antibody, and were analysed by confocal microscopy. Scale bar: 10 µm. (B) Knockdown of Rab39a expression was confirmed by western blotting. Tubulin was used as a loading control. (C) Bar graph shows the yield of infectious particles measured as inclusion-forming units (IFU/ml). Data are representative of three independent experiments (**P*<0.01, Student's *t*-test). (D–F) HeLa cells were transfected with different Rab39a siRNA sequences as described in the Materials and Methods: siRNA (1) Rab39a, siRNA (3) Rab39a or a combination of both (1–3). At 48 h post-transfection, cells were infected with *C. trachomatis* L2 (MOI 5) for 24 h. Next, cells were fixed and bacteria were detected using FITC-coupled anti-MOMP antibody. (D) Knockdown of Rab39a expression was confirmed by western blotting. Tubulin was used as a loading control. (E) Bar graph represents the relative expression level of Rab39a after the transfection with the different siRNAs. Data are representative of three independent experiments. ****P*<0.001, one-way ANOVA and Bonferroni's multiple comparison test. (F) The scatter plot represents the area of inclusions. Each point represents a single inclusion. The mean values are represented with green lines. Data are representative of three independent experiments. ****P*<0.001, one-way ANOVA and Bonferroni's multiple comparison test.

subset of late endocytic vesicles that are acidic, and LAMP1- and LBPA-positive, but do not contain the hydrolytic enzyme cathepsin D (Fig. 4A,B). Proteomic analysis of model phagosomes containing latex beads has depicted sequential acquisition and loss of Rab proteins as the vesicles mature to terminal phagolysosomes (Gutierrez, 2013). Interestingly, Rab39a recruitment follows the same kinetics as that of Rab7 on latex-bead- and *Staphylococcus aureus*-containing phagosomes. *Mycobacterium tuberculosis* arrest phagosome maturation by avoiding the recruitment of Rab39a. Furthermore, Rab39a regulates phagosomal acidification, but it does not participate in the delivery of cathepsin D to the phagosomes (Seto et al., 2011). This latter report is in agreement with our finding that the subset of late endocytic vesicles labelled with Rab39a is not enriched in the hydrolytic enzyme cathepsin D. A key point of our study is the demonstration that Rab39a, a GTPase that controls transport at the late endocytic pathway, is recruited to chlamydial inclusions.

Rab39a is actively recruited to inclusions throughout the entire chlamydial developmental cycle (Fig. 2A; supplementary material Movie 1). Cells infected with dead bacteria or treated with inhibitors of bacterial protein synthesis display individual elementary-body-containing vacuoles, randomly dispersed throughout the cytoplasm, which do not acquire Rab39a (supplementary material Fig. S1B,C). These results are in line with previous reports that indicate that currently unknown chlamydial proteins might supersede recruitment of host Rabs to inclusions (Betts et al., 2009; Dehoux et al., 2011; Valdivia, 2008). In addition, Rab39a association with chlamydial inclusions was confirmed in different cell types and with different *C. trachomatis* serovars (Fig. 1C,D). However, Rab39a is recruited to inclusions in a nucleotide-dependent manner (Fig. 3B). This is also the case for Rab4, Rab6, Rab11 and Rab14 (Capmany and Damiani, 2010; Moorhead et al., 2007; Rzomp et al., 2006).

Live-cell imaging shows that Rab39a-positive vesicles move at a high speed on functional microtubules resulting in a vectorial transport to the inclusion (Fig. 2C; supplementary material Movies 2 and 3). In agreement with recent reports (Al-Zeer et al., 2014; Richards et al., 2013), our results confirm the participation of microtubules in homotypic fusion and enlargement of chlamydial inclusions (Fig. 3C). The recruitment of certain Rabs to chlamydial inclusions might promote selective interactions with host vesicles containing nutrients and structural components beneficial for the bacteria (Damiani et al., 2014).

Journal of Cell Science (2015) 128, 3068-3081 doi:10.1242/jcs.170092

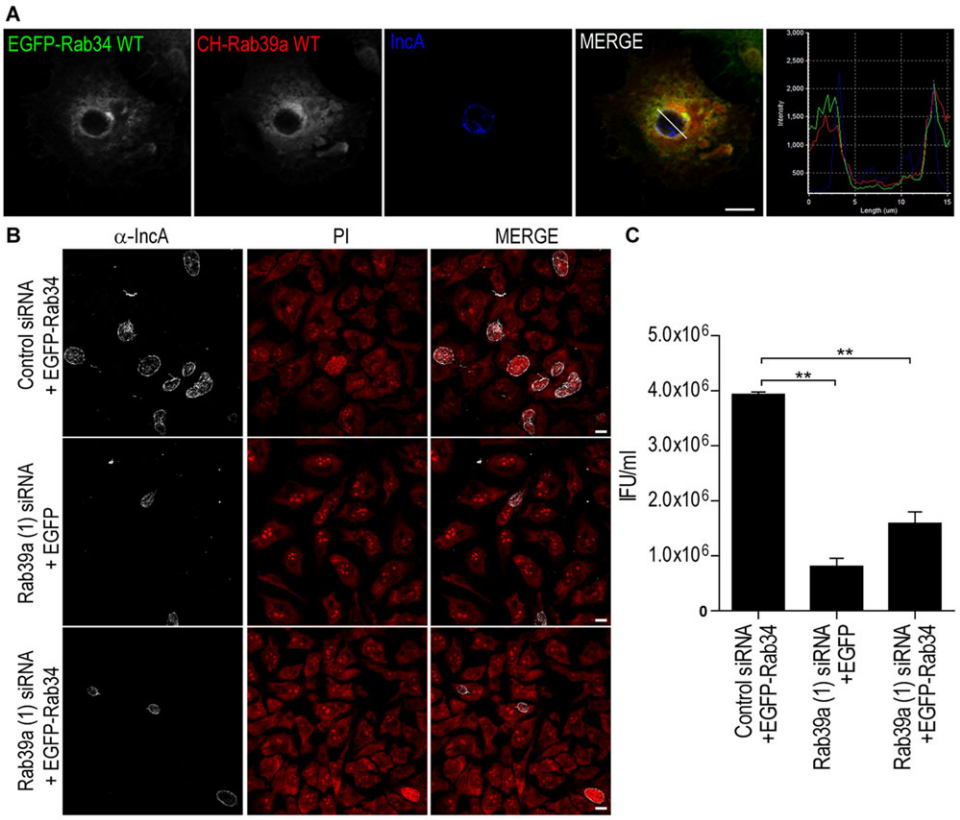

Fig. 8. Impairment of *C. trachomatis* development in Rab39a-depleted cells is not rescued by Rab34. (A) HeLa cells were co-transfected with pEGFP-Rab34 WT (green) and pCherry-Rab39a WT (red) and infected with *C. trachomatis* serovar L2 (MOI 5) for 24 h. IncA was detected with specific antibodies followed by Cy5-conjugated anti-rabbit-IgG antibody (blue). The right panel shows a distribution intensity profile scanned along the line that crosses the inclusion. (B) HeLa cells were transfected with control siRNA or specific Rab39a (1) siRNA as indicated. At 24 h post-transfection, cells were transfected with pEGFP-Rab34 WT (upper and lower panels) or the vector pEGFP (middle panels), and 24 h later, cells were infected with *C. trachomatis* L2 (MOI 5) for 48 h. Images show the inclusions generated by bacterial progenies collected from Rab34-overexpressing cells (upper panels), Rab39a-depleted cells (middle panels) and Rab39a-depleted cells that overexpress Rab34 WT (lower panels). Cells were fixed at 24 hpi and IncA was detected using anti-IncA antibodies followed by Cy5-labelled goat anti-rabbit-IgG antibody. DNA was stained with propidium iodide (PI). Note that overexpression of Rab34 did not overcome the detrimental effect on chlamydial development caused by Rab39a depletion. (C) Cells were treated in a similar way to B, but in this case, the harvested infectious particles (elementary bodies) were titrated, in serial dilution, on HeLa cells to quantify the inclusion-forming units (IFU/ml). Data are representative of three independent experiments. $^{**}P<0.01$, one-way ANOVA and Bonferroni's Multiple comparison test. Scale bars: 10 µm.

One well-established fact is that the growth of *C. trachomatis* heavily relies upon scavenging lipids by the recruitment of lipid factory machineries from cytosol and by the capture of Golgi-derived vesicles, lipid droplets and MVBs from host cells (Beatty, 2006; Cocchiaro et al., 2008; Derré et al., 2011; Elwell et al., 2011; Hackstadt et al., 1996). Actually, MVBs, organelles rich in sphingolipids, phospholipids and cholesterol, are central to intracellular lipid segregation (Denzer et al., 2000; Huotari and Helenius, 2011; Piper and Katzmann, 2007; Stoorvogel et al., 2002; Woodman and Futter, 2008) and are major providers of host-derived lipids to growing inclusions (Beatty, 2006). In addition to their role in exogenous material sorting, MVBs might act as intermediates in the transport of Golgi-derived vesicles (Denzer et al., 2000; Huotari and Helenius, 2011; Piper and Katzmann, 2007; Stoorvogel et al., 2002; Woodman and Futter, 2008). MVBs interact with chlamydial inclusions even in the absence of CD63 (Beatty, 2008). Furthermore, specific inhibitors of sphingomyelin biosynthesis and MVB transport drastically impair chlamydial development, with the loss of inclusion membrane integrity and premature release of few infectious particles (Robertson et al., 2009). Despite the strong requirement of MVBs for bacterial growth, the Rab protein involved in the transport of these late endocytic organelles to the inclusions had not been described until now.

Previous reports have shown that there are lipid droplets and peroxisomes within the inclusion lumen, suggesting the ability of inclusions to 'ingest' host organelles (Bastidas et al., 2013; Boncompain et al., 2014). Ultra-structurally, we recognized intra-inclusion membranes and small vesicles dually labelled with Rab39a and CD63, probably delivered by fusion with MVBs (Fig. 5B; supplementary material Movie 4). Silencing of Rab39a decreases the amount of CD63-labelled vesicles that reaches the inclusion lumen (Fig. 5C) and reduces inclusion growth (Fig. 7F). The unexpected decrease in the size of inclusions developed by progeny collected from Rab39a-depleted cells or cells overexpressing the inactive Rab39a S22N mutant (supplementary material Fig. S4C) suggests that there is a delay in inclusion growth that could be attributed to a defect in the lipid composition of bacteria, impairing the replication processes at initial stages.

Our findings point to a spatial colocalization and functional connection between Rab39a and MVBs, as well as between Rab39a and endogenously synthesized sphingolipids in infected cells (Fig. 6A,B). Using loss-of-function approaches we demonstrate the involvement of Rab39a in MVBs and sphingolipid transport to

Journal of Cell Science (2015) 128, 3068-3081 doi:10.1242/jcs.170092

chlamydial inclusions (Fig. 6C). Furthermore, interfering with Rab39a function impairs the yield of infectious bacteria, as shown by IFU assays (Fig. 7C; supplementary material Fig. S4B). Similar to what happens after silencing other Rabs, bacterial replication and infectivity is reduced but not suppressed (Capmany and Damiani, 2010; Rejman Lipinski et al., 2009). Despite the fact that Rab39 is a short variant of Rab34, the detrimental impact on *C. trachomatis* propagation caused by Rab39a depletion, could not be overcome by overexpression of Rab34 (Fig. 8B,C). Taken together, these results support the notion that these bacteria simultaneously exploit distinct trafficking pathways to ensure their growth and replication. Among them, our findings demonstrate that *C. trachomatis* hijack Rab39a-mediated trafficking to favour their intracellular development.

Our findings are shedding light on strategies developed by *C. trachomatis* to acquire nutrients from host cells, including the re-routing of MVBs to the inclusions. Further research is needed to fully understand the molecular mechanisms involved in MVB–inclusion interaction. Nevertheless, the identification of a Rab GTPase that participates in trafficking from late endocytic organelles to the chlamydial inclusion constitutes a substantial step in unravelling the interplay between *C. trachomatis* and host cells.

MATERIALS AND METHODS

Cell culture and *C. trachomatis* propagation

Human epithelial HeLa 229 cells, HFF cells or CHO cells (ABAC, Buenos Aires, Argentina) were cultured in infection medium at 37°C with 5% CO_2 and 95% humidified air. Infection medium contains high-glucose Dulbecco's modified Eagle's medium (DMEM; GIBCO-BRL, Buenos Aires, Argentina) supplemented with 10% fetal bovine serum (FBS) (Internegocios SA, Buenos Aires, Argentina), 0.3 mg/ml L-glutamine (ICN Biomedicals Inc, OH) and 1.55 mg/ml glucose (Biopack, Buenos Aires, Argentina), without antibiotics. Opti-MEM (Invitrogen, Buenos Aires, Argentina) was used for transfection. *Chlamydia trachomatis* serovar L2 and serovar D were donated and typified by the Unidad de Estudios de *Chlamydias* (Facultad de Farmacia y Bioquímica, Universidad de Buenos Aires, Argentina). *C. trachomatis* transformed strains harbouring p2TK2-SW2 IncDProm-mCherry-IncDTerm were generated and kindly provided by Agaisse and Derré (Agaisse and Derré, 2013). For bacterial propagation, HeLa cells were infected at a multiplicity of infection (MOI) of 20 and incubated for 48 h. Then, infected cells were lysed using Hanks' solutions with glass beads and elementary bodies were purified by centrifugation as previously described (Caldwell et al., 1981). The purified elementary bodies were suspended in 0.2 M sucrose, L-glutamine and 0.2 M phosphate buffer (SPG; pH 7.2) and titrated by determination of inclusion-forming units (IFUs).

Plasmids, antibodies and reagents

The plasmids pEGFP-Rab7a WT, pEGFP-Rab34 WT, pEGFP-Rab39a WT, pEGFP-Rab39a Q72L and pEGFP-Rab39a S22N were constructed in our laboratories. The primary antibodies used were: mouse monoclonal anti-GM130, anti-TGN46 and anti-LAMP1 from BD Biosciences (MI); anti-tubulin, anti-actin, anti-Rab5 and anti-GFP from Abcam (MI); anti-cathepsin D from Aviva systems biology (MI); FITC-coupled anti-MOMP antibody from Dakocytomation (Ely, UK); anti-*C. trachomatis* IncG, anti-IncA and anti-elementary-body antibody generously provided by David Hackstadt (National Institute of Allergy and Infectious Diseases, Hamilton, MT); anti-CD63 from Zymed (Invitrogen, France); anti-LBPA given by Laura Delgui (IHEM, Mendoza, Argentina); and rabbit polyclonal anti-Rab39a antibody, made at our laboratory. The secondary antibodies were: goat Cy3-labelled anti-rabbit-IgG, goat Cy3-labelled anti-mouse-IgG, goat horseradish peroxidase (HRP)-conjugated anti-rabbit-IgG and goat HRP-conjugated anti-mouse-IgG antibodies purchased from Jackson ImmunoResearch Laboratories (West Grove, PA). LysoTracker Red DND-99, Hoechst 33342, propidium iodide and DAPI were from Molecular Probes (Life Technologies, Buenos Aires, Argentina); nocodazole and Mowiol were from Calbiochem (San Diego, CA) and brefeldin A (BFA), chloramphenicol and dimethyl sulfoxide (DMSO) were from Merck (Buenos Aires, Argentina).

Cell transfection

HeLa 229 cells were grown on 12-mm-diameter glass cover slips in 24-well plates (ETC internacional, Buenos Aires, Argentina) until 70% confluence. Cells were washed once with serum-free DMEM (GIBCO-BRL Buenos Aires, Argentina) and transfected with XtremeGene 9 (Roche Applied Science, Indianapolis, IN) or Lipofectamine 2000 (Invitrogen, Buenos Aires, Argentina) using 1 µl per 1 µg of DNA per well according to the manufacturers' protocol. For silencing assays, siRNA was transfected with Ribocellin transfection reagent (BioCellinChallenge, SAS, France). All siRNA oligonucleotides targeting Rab39a were purchased from Thermo scientific (Thermo, Paris, France) and the sequences used were 5′-AAUC-UUGACGAGAGACAUA-3′ (1) and 5′-CAGGAGCGGUUCAGAUC-AA-3′ (3). In all cases a siRNA oligonucleotide targeting firefly luciferase (siLuc) was used as a control.

Infection and detection of *C. trachomatis*

HeLa cells transfected with pEGFP-Rab39a were infected 18 h later by diluting bacterial stock in infection medium. Cells were centrifuged (450 ***g***, 15 min, room temperature) to synchronize the infection and then incubated for the internalization step (120 min, 37°C and 5% CO_2). After that, cells were washed two times with phosphate-buffered saline (PBS) to eliminate non-internalized bacteria, and finally, cells were incubated in the presence of infection medium for the indicated post infection times (hpi). *C. trachomatis* was detected using DNA stains (DAPI, propidium iodide or Hoechst 33342) or antibodies such as rabbit anti-elementary-body or FITC-coupled anti-MOMP antibody.

Immunofluorescence and confocal microscopy

For colocalization studies, HeLa cells were grown on cover slips in 24-well plates and transfected with the chosen plasmid at least 24 h before the experiment, and then, cells were infected with *C. trachomatis* according to the assay. To detect endogenous proteins, infected cells were fixed in 3% paraformaldehyde (PFA) in PBS for 20 min at room temperature. Aldehydes were quenched with 50 mM NH_4Cl for 5 min. Cells were washed in PBS and permeabilized with 0.2% saponin and 1 mg/ml BSA in PBS. After that, cells were incubated for 60 min with the appropriate primary antibody followed by incubation with a fluorescently labelled secondary antibody. Coverslips were mounted in Mowiol containing 0.5 µg/ml Hoechst 33342 or DAPI for DNA staining. Optical sections of 0.21 µm thickness were acquired for 3D reconstructions. Distribution intensity profiles were performed and analysed with FV10 software (Olympus America, Inc., Melville, NY). The size of the inclusion was determined as pixel area in a middle *z*-plane. An Olympus FV-1000 spectral confocal unit mounted on an IX-25 Olympus inverted microscope was used. Images were acquired and analysed with FV10-ASW 1.7 Software, and then processed using ImageJ and Adobe Illustrator CS3 software.

Time-lapse fluorescence microscopy

Transfected cells were grown on glass-bottomed 35-mm dishes (Iwaki; Asahi Techno Glass, Tokyo, Japan). Time-lapse imaging was performed at 37°C on a spinning-disk confocal microscope mounted on an inverted motorized microscope (DMIRE2; Leica, Wetzlar, Germany) equipped with a CSUXI spinning disk head (Yokogawa, Tokyo, Japan) and temperature and CO_2 controller (Life Imaging Services, Reinach, Switzerland). Images were captured on a QuantEM 512SC camera (Photometrics). A *z*-stack of three planes was acquired every 1 s for a period of 1 min. Movies were generated using MetaMorph software (NY).

Immunoelectron microscopy

Cell samples were fixed in a mixture of 2% PFA and 0.125% glutaraldehyde in a 0.1 M phosphate buffer pH 7.4 and processed for ultracryomicrotomy as described previously (Raposo et al., 1997). Ultrathin sections were prepared with an ultracryomicrotome Ultracut FCS (Leica) and underwent single or double immunogold labelling with protein A conjugated to gold particles 10 nm or 15 nm in diameter (Cell Microscopy Center, Department of Cell

Biology, Utrecht University). EGFP–Rab39a was detected with the appropriate antibodies (from Molecular Probes) and then labelled using protein A conjugated to 10-nm gold particles (PA-G10). CD63 was detected with primary antibodies (from Zymed) followed by anti-mouse-IgG, and labelled using protein A conjugated to 15-nm gold particles (PA-G15) as reported previously (Theos et al., 2005). Sections were analysed on a Tecnai Spirit G2 electron microscope (FEI, Eindhoven, The Netherlands) and digital acquisitions were made with a 4k CCD camera (Quemesa, Olympus, Münster, Germany).

RNA interference

2.5×10^5 cells were seeded onto six-well tissue culture plates and 24 h later were transfected with control (2 nM of luciferase control siRNA) or Rab39a-specific (2 nM of a mix of predesigned siRNA directed against human RAB39A) siRNA, using Ribocellin transfection reagent and Opti-MEM accordingly to the siRNA transfection protocol suggested by the manufacturer. At 48 h post transfection, cells were infected with *C. trachomatis*. After 2 days, the amount of infectious particles was measured by IFU assays.

Immunoblotting

Cell lysates were resolved by western blotting. Protein levels were quantified using a bicinchoninic acid (BCA) protein assay kit (Pierce™ Thermo Scientific). Equal amounts of proteins were separated in 12% gradient SDS-PAGE gels. Separated proteins were transferred onto nitrocellulose membranes and then detected using polyclonal rabbit anti-Rab39a (1:50) followed by goat HRP-conjugated anti-rabbit-IgG antibodies (1:5000). Protein loading was controlled with monoclonal mouse anti-tubulin (1:1000) or anti-actin (1:1000) and goat HRP-labelled anti-mouse-IgG antibodies (1:5000). An Amersham ECL Plus™ kit was used to detect HRP activity (GE Healthcare Life Sciences, Buenos Aires, Argentina).

IFU assays

Transfected cells were infected with *C. trachomatis* L2 for 48 h, lysed with glass beads in SPG buffer and titrated on HeLa cells. Cell lysates were centrifuged for 10 min at 500 ***g*** to remove debris and progressive dilutions were inoculated onto HeLa cells seeded on 24-well plates. After 24 h, cells were fixed, permeabilized and the bacteria were stained with FITC-coupled anti-MOMP antibody or another specific antibody. The numbers of inclusions formed by chlamydial progeny were counted in 30 fields by microscopical analysis and expressed as IFUs per ml.

Statistical analysis

The data represent the mean±s.e.m. of n experiments. For simple paired analyses between two groups, a Student's t-test was chosen. For multiple comparisons, ANOVA with subsequent Bonferroni's test was used. A P value less than 0.01 was considered to be statistically significant.

Acknowledgements

We thank I. Derré (Yale University, USA) and A. Subtil (Pasteur Institute, Paris, France) for the fluorescent bacteria, and T. Hackstadt (Rocky Mountains Laboratories, USA) for the anti-Incs and anti-elementary-body antibodies. We thank L. Delgui (IHEM, Argentina) and J. Cordero (University of Glasgow, UK) for helpful criticisms on this work. We acknowledge the Investments for the Future program (France-BioImaging, ANR-10-INSB-04), PICT-IBiSA (CelTisPhyBio Labex, number ANR-10-LBX-0038) and IDEX PSL (number ANR-10-IDEX-0001-02 PSL) for the use of electron microscopy facility.

Competing interests

The authors declare no competing or financial interests.

Author contributions

J.G.T. and M.T.D. conceived and designed the experiments. J.G.T. and A.C. performed the experiment. C.Q. generated Rab39a constructs. A.C, M.R. and G.R. performed EM. J.G.T, S.M.-L, B.G. and M.T.D. analysed the data. J.G.T and M.T.D. wrote the paper.

Funding

This work was supported by Agencia Nacional de Ciencia y Tecnología [grant number PICT 2116 to M.T.D.]; Consejo Nacional de Investigaciones Científicas y Técnicas (grant PIP to M.T.D.); and Secretaría de Ciencia, Técnica y Postgrado de la Universidad Nacional de Cuyo (grant Sectyp to M.T. D.). We acknowledge the Mincyt-Ecos Sud [grant number A11S03] support to B.G. and M.T.D.

Supplementary material

Supplementary material available online at
http://jcs.biologists.org/lookup/suppl/doi:10.1242/jcs.170092/-/DC1

References

Agaisse, H. and Derré, I. (2013). A C. trachomatis cloning vector and the generation of C. trachomatis strains expressing fluorescent proteins under the control of a C. trachomatis promoter. *PLoS ONE* **8**, e57090.

Ali, B. R. and Seabra, M. C. (2005). Targeting of Rab GTPases to cellular membranes. *Biochem. Soc. Trans.* **33**, 652-656.

Al-Zeer, M. A, Al-Younes, H. M., Kerr, M., Abu-Lubad, M., Gonzalez, E., Brinkmann, V. and Meyer, T. F. (2014). Chlamydia trachomatis remodels stable microtubules to coordinate Golgi stack recruitment to the chlamydial inclusion surface. *Mol. Microbiol.* **94**, 1285-1297.

Bastidas, R. J., Elwell, C. A, Engel, J. N. and Valdivia, R. H. (2013). Chlamydial intracellular survival strategies. *Cold Spring Harb. Perspect. Med.* **3**, a010256.

Beatty, W. L. (2006). Trafficking from CD63-positive late endocytic multivesicular bodies is essential for intracellular development of Chlamydia trachomatis. *J. Cell Sci.* **119**, 350-359.

Beatty, W. L. (2008). Late endocytic multivesicular bodies intersect the chlamydial inclusion in the absence of CD63. *Infect. Immun.* **76**, 2872-2881.

Becker, C. E., Creagh, E. M. and O'Neill, L. A J. (2009). Rab39a binds caspase-1 and is required for caspase-1-dependent interleukin-1beta secretion. *J. Biol. Chem.* **284**, 34531-34537.

Betts, H. J., Wolf, K. and Fields, K. A. (2009). Effector protein modulation of host cells: examples in the Chlamydia spp. arsenal. *Curr. Opin. Microbiol.* **12**, 81-87.

Boncompain, G., Müller, C., Meas-Yedid, V., Schmitt-Kopplin, P., Lazarow, P. B. and Subtil, A. (2014). The intracellular bacteria Chlamydia hijack peroxisomes and utilize their enzymatic capacity to produce bacteria-specific phospholipids. *PLoS ONE* **9**, e86196.

Caldwell, H. D. and Kromhout, J. (1981). Schachter Purification and partial characterization of the major outer membrane protein of Chlamydia trachomatis. *J. Infect Immun.* **31**, 1161-1176.

Capmany, A. and Damiani, M. T. (2010). Chlamydia trachomatis intercepts Golgi-derived sphingolipids through a Rab14-mediated transport required for bacterial development and replication. *PLoS ONE* **5**, e14084.

Capmany, A., Leiva, N. and Damiani, M. T. (2011). Golgi-associated Rab14, a new regulator for Chlamydia trachomatis infection outcome. *Commun. Integr. Biol.* **4**, 590-593.

Chen, T., Han, Y., Yang, M., Zhang, W., Li, N., Wan, T., Guo, J. and Cao, X. (2003). Rab39, a novel Golgi-associated Rab GTPase from human dendritic cells involved in cellular endocytosis. *Biochem. Biophys. Res. Commun.* **303**, 1114-1120.

Cocchiaro, J. L., Kumar, Y., Fischer, E. R., Hackstadt, T. and Valdivia, R. H. (2008). Cytoplasmic lipid droplets are translocated into the lumen of the Chlamydia trachomatis parasitophorous vacuole. *Proc. Natl. Acad. Sci. USA* **105**, 9379-9384.

Damiani, M. T., Gambarte Tudela, J. and Capmany, A. (2014). Targeting eukaryotic Rab proteins: a smart strategy for chlamydial survival and replication. *Cell. Microbiol.* **16**, 1329-1338.

Dehoux, P., Flores, R., Dauga, C., Zhong, G. and Subtil, A. (2011). Multi-genome identification and characterization of chlamydiae-specific type III secretion substrates: the Inc proteins. *BMC Genomics* **12**, 109.

Denzer, K., Kleijmeer, M. J., Heijnen, H. F., Stoorvogel, W. and Geuze, H. J. (2000). Exosome: from internal vesicle of the multivesicular body to intercellular signaling device. *J. Cell Sci.* **113**, 3365-3374.

Derré, I., Swiss, R. and Agaisse, H. (2011). The lipid transfer protein CERT interacts with the Chlamydia inclusion protein IncD and participates to ER-Chlamydia inclusion membrane contact sites. *PLoS Pathog.* **7**, e1002092.

Elwell, C. A., Jiang, S., Kim, J. H., Lee, A., Wittmann, T., Hanada, K., Melancon, P. and Engel, J. N. (2011). Chlamydia trachomatis co-opts GBF1 and CERT to acquire host sphingomyelin for distinct roles during intracellular development. *PLoS Pathog.* **7**, e1002198.

Fields, K. A. and Hackstadt, T. (2002). The chlamydial inclusion: escape from the endocytic pathway. *Annu. Rev. Cell Dev. Biol.* **18**, 221-245.

Fukuda, M., Kanno, E., Ishibashi, K. and Itoh, T. (2008). Large scale screening for novel rab effectors reveals unexpected broad Rab binding specificity. *Mol. Cell. Proteomics* **7**, 1031-1042.

Giannandrea, M., Bianchi, V., Mignogna, M. L., Sirri, A., Carrabino, S., D'Elia, E., Vecellio, M., Russo, S., Cogliati, F., Larizza, L. et al. (2010). Mutations in the small GTPase gene RAB39B are responsible for X-linked mental retardation associated with autism, epilepsy, and macrocephaly. *Am. J. Hum. Genet.* **86**, 185-195.

Grieshaber, S. S., Grieshaber, N. A. and Hackstadt, T. (2003). Chlamydia trachomatis uses host cell dynein to traffic to the microtubule-organizing center in a p50 dynamitin-independent process. *J. Cell Sci.* **116**, 3793-3802.
Gutierrez, M. G. (2013). Functional role(s) of phagosomal Rab GTPases. *Small GTPases* **4**, 148-158.
Hackstadt, T., Rockey, D. D., Heinzen, R. A. and Scidmore, M. A. (1996). Chlamydia trachomatis interrupts an exocytic pathway to acquire endogenously synthesized sphingomyelin in transit from the Golgi apparatus to the plasma membrane. *EMBO J.* **15**, 964-977.
Heinzen, R. A., Scidmore, M. A., Rockey, D. D. and Hackstadt, T. (1996). Differential interaction with endocytic and exocytic pathways distinguish parasitophorous vacuoles of Coxiella burnetii and Chlamydia trachomatis. *Infect. Immun.* **64**, 796-809.
Huotari, J. and Helenius, A. (2011). Endosome maturation. *EMBO J.* **30**, 3481-3500.
Kobayashi, T., Vischer, U. M., Rosnoblet, C., Lebrand, C., Lindsay, M., Parton, R. G., Kruithof, E. K. O. and Gruenberg, J. (2000). The tetraspanin CD63/lamp3 cycles between endocytic and secretory compartments in human endothelial cells. *Mol. Biol. Cell* **11**, 1829-1843.
Leiva, N., Capmany, A. and Damiani, M. T. (2013). Rab11-family of interacting protein 2 associates with chlamydial inclusions through its Rab-binding domain and promotes bacterial multiplication. *Cell. Microbiol.* **15**, 114-129.
Mignogna, M. L., Giannandrea, M., Gurgone, A., Fanelli, F., Raimondi, F., Mapelli, L., Bassani, S., Fang, H., Van Anken, E., Alessio, M. et al. (2015). The intellectual disability protein RAB39B selectively regulates GluA2 trafficking to determine synaptic AMPAR composition. *Nat. Commun.* **6**, 6504.
Moore, E. R., Fischer, E. R., Mead, D. J. and Hackstadt, T. (2008). The chlamydial inclusion preferentially intercepts basolaterally directed sphingomyelin-containing exocytic vacuoles. *Traffic* **9**, 2130-2140.
Moorhead, A. R., Rzomp, K. A. and Scidmore, M. A. (2007). The Rab6 effector Bicaudal D1 associates with Chlamydia trachomatis inclusions in a biovar-specific manner. *Infect. Immun.* **75**, 781-791.
Mori, Y., Matsui, T., Omote, D. and Fukuda, M. (2013). Small GTPase Rab39A interacts with UACA and regulates the retinoic acid-induced neurite morphology of Neuro2A cells. *Biochem. Biophys. Res. Commun.* **435**, 113-119.
Ouellette, S. P., Dorsey, F. C., Moshiach, S., Cleveland, J. L. and Carabeo, R. A. (2011). Chlamydia species-dependent differences in the growth requirement for lysosomes. *PLoS ONE* **6**, e16783.
Piper, R. C. and Katzmann, D. J. (2007). Biogenesis and function of multivesicular bodies. *Annu. Rev. Cell Dev. Biol.* **23**, 519-547.
Raposo, G., Kleijmeer, M. J., Posthuma, G., Slot, J. W. and Geuze, H. J. (1997). Immunogold labeling of ultrathin cryosections: application in immunology. In *Handbook of Experimental Immunology in Four Volumes*, Vol. 4 (ed. D. M. Weir, L. A. Herzenberg, and C. Blackwell), pp. 1-11. Cambridge: Blackwell Science.
Rejman Lipinski, A., Heymann, J., Meissner, C., Karlas, A., Brinkmann, V., Meyer, T. F. and Heuer, D. (2009). Rab6 and Rab11 regulate Chlamydia trachomatis development and golgin-84-dependent Golgi fragmentation. *PLoS Pathog.* **5**, e1000615.
Richards, T. S., Knowlton, A. E. and Grieshaber, S. S. (2013). Chlamydia trachomatis homotypic inclusion fusion is promoted by host microtubule trafficking. *BMC Microbiol.* **13**, 185.
Robertson, D. K., Gu, L., Rowe, R. K. and Beatty, W. L. (2009). Inclusion biogenesis and reactivation of persistent Chlamydia trachomatis requires host cell sphingolipid biosynthesis. *PLoS Pathog.* **5**, e1000664.
Rzomp, K. A., Scholtes, L. D., Briggs, B. J., Whittaker, G. R. and Scidmore, M. A. (2003). Rab GTPases are recruited to chlamydial inclusions in both a species-dependent and species-independent manner. *Infect. Immun.* **71**, 5855-5870.
Rzomp, K. A., Moorhead, A. R. and Scidmore, M. A. (2006). The GTPase Rab4 interacts with Chlamydia trachomatis inclusion membrane protein CT229. *Infect. Immun.* **74**, 5362-5373.
Saka, H. A. and Valdivia, R. H. (2010). Acquisition of nutrients by Chlamydiae: unique challenges of living in an intracellular compartment. *Curr. Opin. Microbiol.* **13**, 4-10.
Savina, A., Fader, C. M., Damiani, M. T. and Colombo, M. I. (2005). Rab11 promotes docking and fusion of multivesicular bodies in a calcium-dependent manner. *Traffic* **6**, 131-143.
Scidmore, M. A., Fischer, E. R. and Hackstadt, T. (2003). Restricted fusion of Chlamydia trachomatis vesicles with endocytic compartments during the initial stages of infection. *Infect. Immun.* **71**, 973-984.
Seto, S., Tsujimura, K. and Koide, Y. (2011). Rab GTPases regulating phagosome maturation are differentially recruited to mycobacterial phagosomes. *Traffic* **12**, 407-420.
Seto, S., Sugaya, K., Tsujimura, K., Nagata, T., Horii, T. and Koide, Y. (2013). Rab39a interacts with phosphatidylinositol 3-kinase and negatively regulates autophagy induced by lipopolysaccharide stimulation in macrophages. *PLoS ONE* **8**, e83324.
Stenmark, H. (2009). Rab GTPases as coordinators of vesicle traffic. *Nat. Rev. Mol. Cell Biol.* **10**, 513-525.
Stoorvogel, W., Kleijmeer, M. J., Geuze, H. J. and Raposo, G. (2002). The biogenesis and functions of exosomes. *Traffic* **3**, 321-330.
Taraska, T., Ward, D. M., Ajioka, R. S., Wyrick, P. B., Davis-Kaplan, S. R., Davis, C. H. and Kaplan, J. (1996). The late chlamydial inclusion membrane is not derived from the endocytic pathway and is relatively deficient in host proteins. *Infect. Immun.* **64**, 3713-3727.
Theos, A. C., Tenza, D., Martina, J. A., Hurbain, I., Peden, A. A., Sviderskaya, E. V., Stewart, A., Robinson, M. S., Bennett, D. C., Cutler, D. F. et al. (2005). Functions of adaptor protein (AP)-3 and AP-1 in tyrosinase sorting from endosomes to melanosomes. *Mol. Biol. Cell* **16**, 5356-5372.
Valdivia, R. H. (2008). Chlamydia effector proteins and new insights into chlamydial cellular microbiology. *Curr. Opin. Microbiol.* **11**, 53-59.
Woodman, P. G. and Futter, C. E. (2008). Multivesicular bodies: co-ordinated progression to maturity. *Curr. Opin. Cell Biol.* **20**, 408-414.
Zerial, M. and McBride, H. (2001). Rab proteins as membrane organizers. *Nat. Rev. Mol. Cell Biol.* **2**, 107-117.

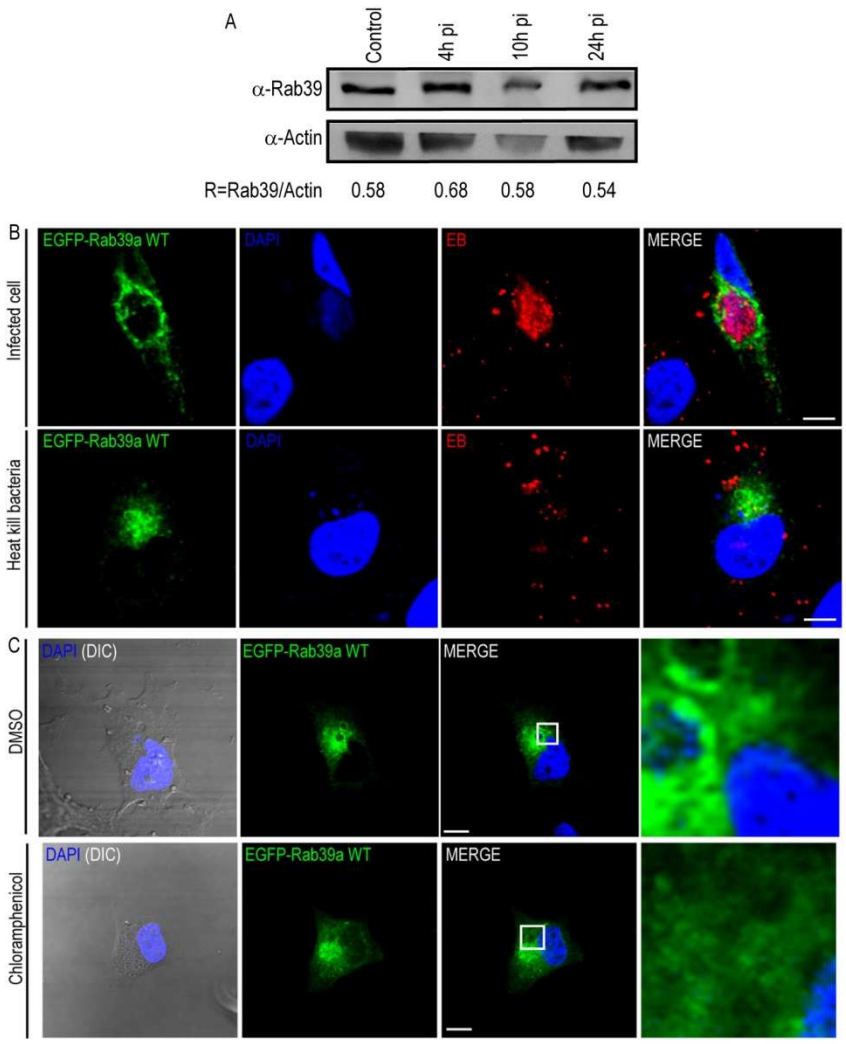

Figure S1. Rab39a recruitment is driven by the bacterium. A) A western blot of lysates of HeLa cells infected with *C. trachomatis* serovar L2 (MOI of 5) for the indicated time p.i. Endogenous Rab39a was detected using rabbit anti-Rab39a followed by goat anti-rabbit HRP-coupled IgG. Actin was used as loading control. Blot representative from 3 independent experiments. B) HeLa cells overexpressing EGFP-Rab39a WT (green) were incubated with live or dead *C. trachomatis* L2 (MOI 5) for 24 h. Bacteria were labeled with rabbit anti-EB antibody followed by goat anti-rabbit Cy3-labelled IgG (red). C) HeLa cells were transfected with pEGFP-Rab39a WT (green) and 24 h later were infected with *C. trachomatis* serovar L2 (MOI 5). After the internalization period (2 h), DMSO (control) or 20 μg/mL chloramphenicol were added. Cells were fixed at 12 h pi. DNA was labelled with DAPI (blue). Insets show a magnification of the selected area. Scale bar, 10 μm.

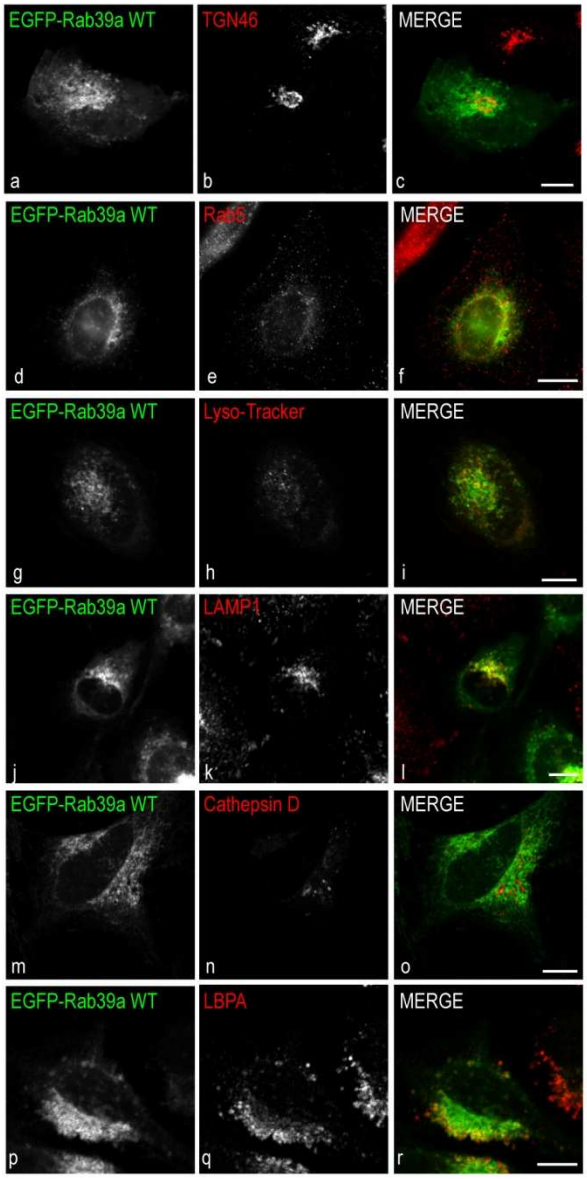

Figure S2. EGFP-Rab39a localizes at late endocytic compartments in uninfected cells. HeLa cells transiently overexpressing EGFP-Rab39a (green) were stained with markers of different subcellular structures: TGN46 (for Trans Golgi network, a-c), Rab5 (for early endosomes, d-f), Lyso-Tracker (for acidic compartments, g-i), LAMP-1 (for late endosomes and lysosomes, j-l), Cathepsin D (for hydrolytic enzymes, m-o), LBPA (for multivesicular bodies, p-r). As indicated, cells were incubated with Lyso-Traker (red) for 10 minutes prior fixation or inmunolabelled with the appropriate primary antibodies followed by goat anti mouse Cy3-labelled IgG (red). Scale bar, 10 μm. Images are representative of two independent experiments.

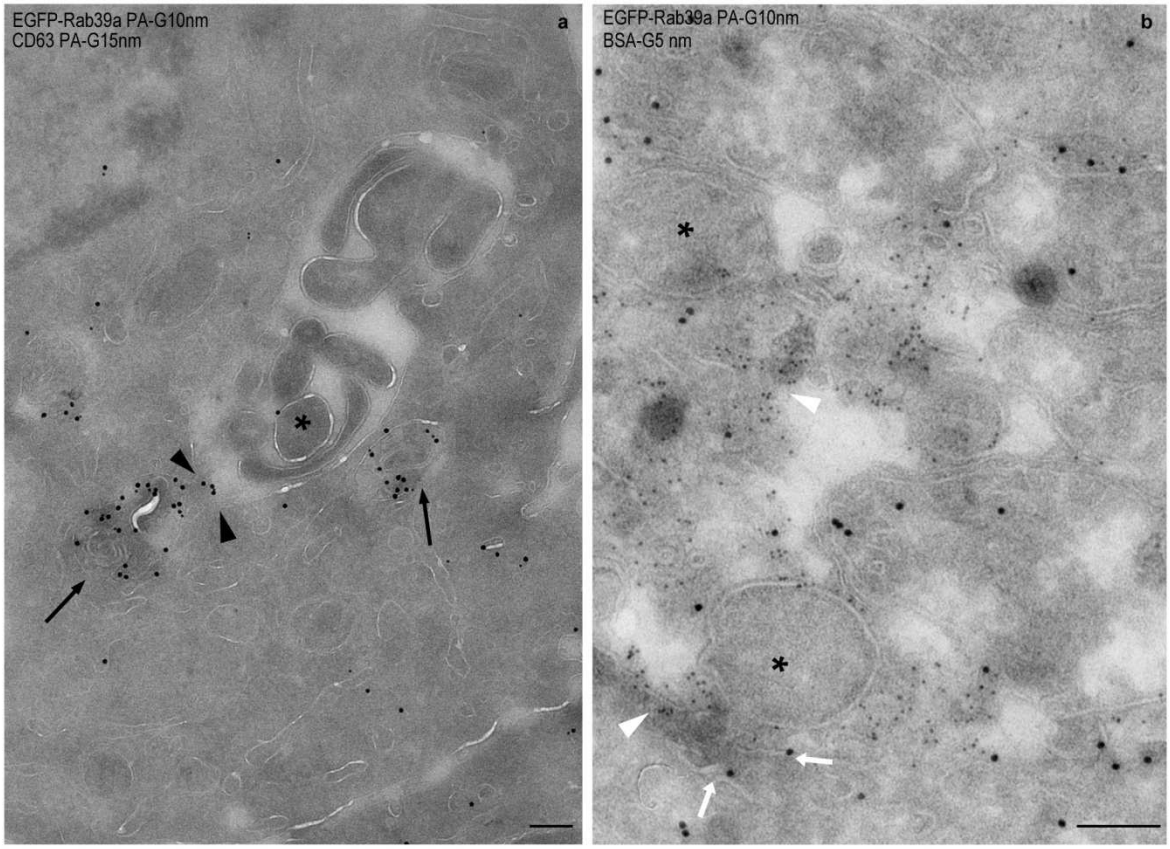

Figure S3. Late endocytic compartments interact with chlamydial inclusions. Panel a: Ultrathincryosections of *C. trachomatis*-infected cells (MOI 1, 24 h) were double immunogold labelled for CD63 (PA-G15) and Rab39a (PA-G10). Several multivesicular bodies (MVBs) labelled for CD63 and Rab39a were in close contact with the chlamydial inclusion membrane (black arrows). A CD63-Rab39a positive MVB was probably undergoing fusion with the chlamydial inclusion (black arrowheads). Bacteria were pointed out with asterisks. Scale bar, 200 nm. Panel b: HeLa cells overexpressing EGFP-Rab39a WT infected with *C. trachomatis* L2 (MOI 1, 24 h) internalized albumin coupled to 5 nm gold (BSA-G5) for 60 minutes. Note the presence of albumin within inclusion lumen (white arrowheads). Rab39a was found associated with inclusion membrane and within inclusion lumen (white arrows). Scale bar, 200 nm.

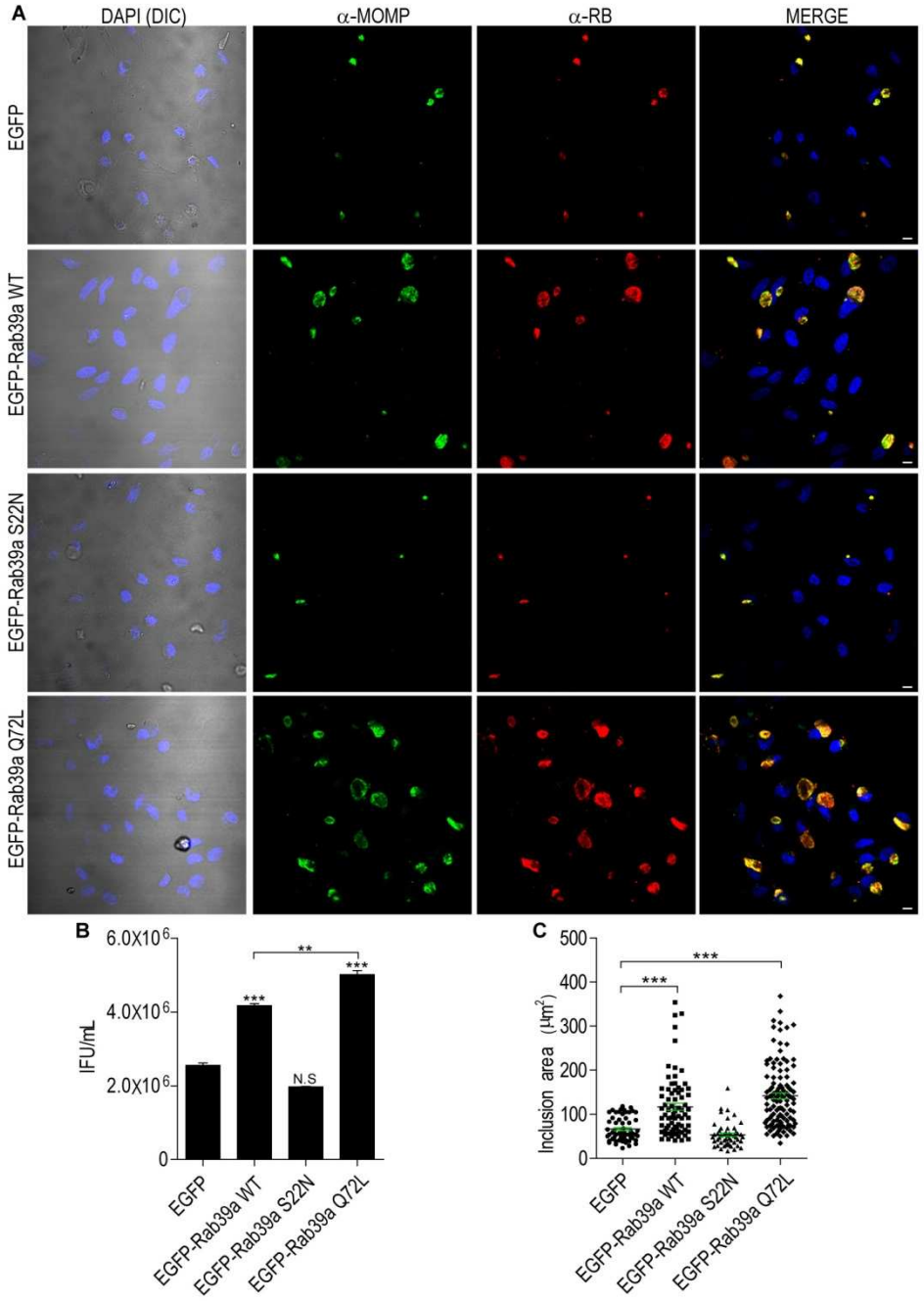

Figure S4. EGFP-Rab39a WT and its GTP-bound mutant EGFP-Rab39a Q72L increase bacterial progeny. A) HeLa cells were transfected with pEGFP, pEGFP-Rab39a WT, pEGFP-Rab39a S22N or pEGFP-Rab39a Q72L, and 24 h later, cells were infected with *C. trachomatis* serovar L2 (MOI 5). The infected cells were lysed after 48 h and the infectious particles (EBs) were titrated, in serial dilution, on HeLa cells. At 24 h pi, *C. trachomatis* were detected using FITC-coupled anti-MOMP IgG (green) and anti-EB antibodies followed by goat anti-mouse Cy3-labelled IgG (red). Scale bar, 10 μm. B) The column bar graph represents the amount of infectious particles measured as IFUs/mL. Data are representative of two independent experiments (***p_0.01, student's t test). C) The scatter plot represents inclusions size. Each point represents a single inclusion. The mean values are represented with green lines. The data are representative of two independent experiments (***p_0.01, student's t test).

Movies

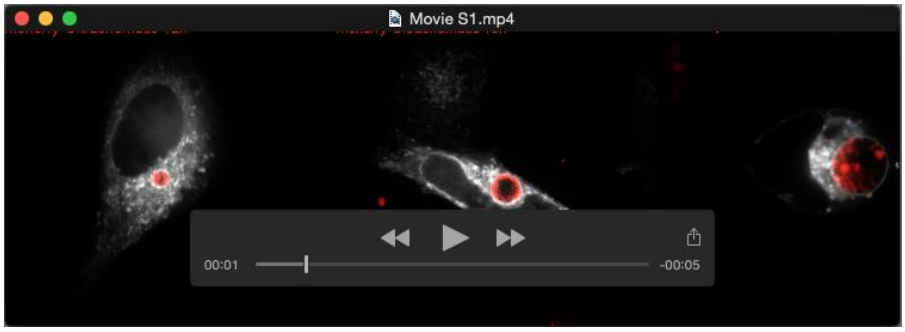

Movie 1. Rab39a-labelled vesicles interact with chlamydial inclusions. HeLa cells transiently overexpressing EGFP-Rab39a WT were infected with *C. trachomatis* transformed strains *harboring* p2TK2-SW2 IncDProm-mCherry-IncDTerm (mCherry) for 12 h, 18 h and 24 h, respectively. Time lapse images were acquired every second by spinning disk microscopy during one minute.

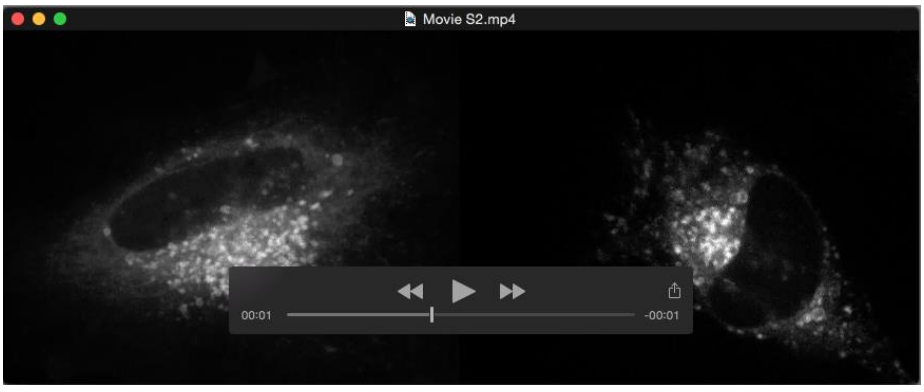

Movie 2. Rab39a-labelled vesicles move along microtubules. HeLa cells transiently overexpressing EGFP-Rab39a were incubated with DMSO (control condition, left panel) or 10 µM Nocodazole for a period of 1 h (right panel). Time lapse images were acquired every second by spinning disk microscopy during 30 s.

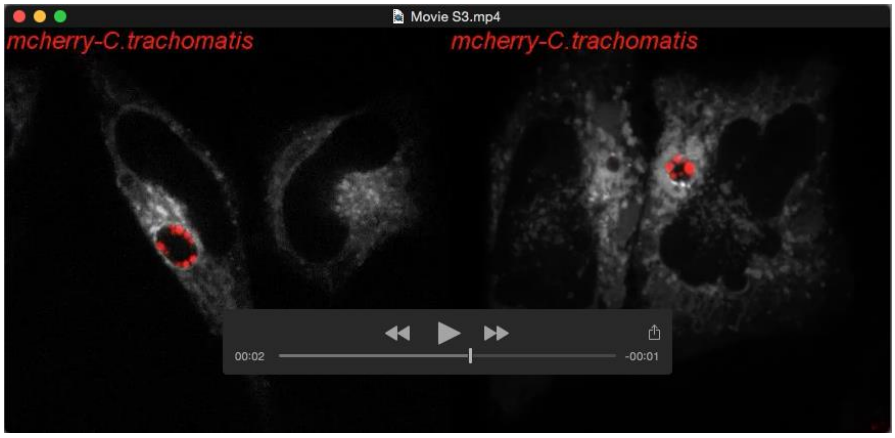

Movie 3. Depolymerization of microtubules interferes with the transport of Rab39a-labelled vesicles to the chlamydial inclusion. HeLa cells transiently overexpressing EGFP-Rab39a were infected with *C. trachomatis* transformed strains harboring p2TK2-SW2 IncDProm-mCherry-IncDTerm (mCherry). Cells were incubated with DMSO (control condition, left panel) or 10 µM Nocodazole for a period of 1 h (right panel). Time lapse images were acquired every second by spinning disk microscopy during one minute.

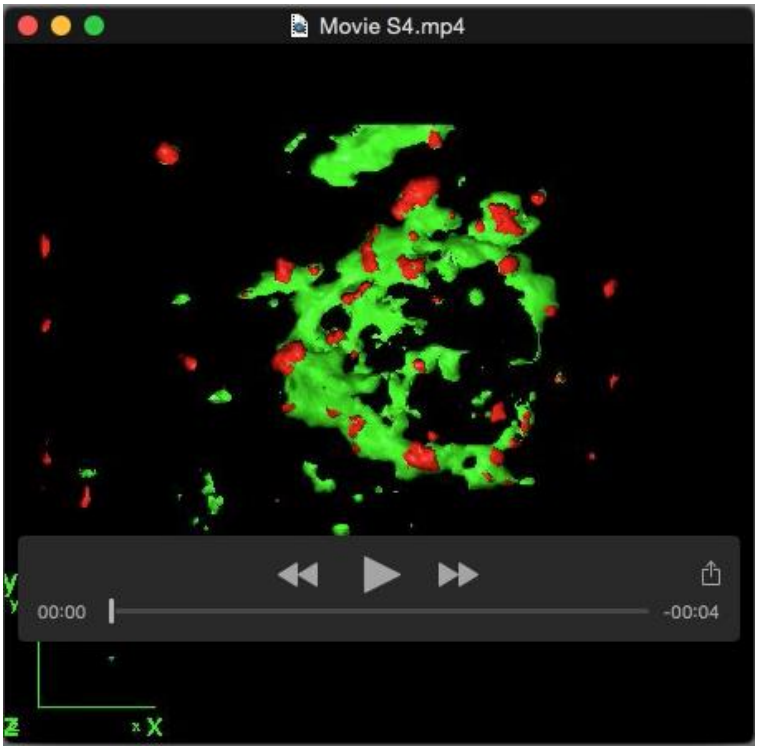

Movie 4. 3D-reconstruction of an infected cell. HeLa cells overexpressing EGFP-Rab39a (green) were infected with *C. trachomatis* serovar L2 (MOI 5) for 24 h. Cells were fixed and multivesicular bodies were identified by immunodetecting CD63 with the appropriate primary antibody followed by goat anti-mouse Cy3-labelled IgG (red). Optical z-sections of 0.21 µm were acquired and used to reconstruct the entire thickness of the cell. ImageJ software was used to build the 3D image.